SEDIMENTOLOGY the journal of the International Association of Sedimentologists

Sedimentology (2017) **64**, 16–43 doi: 10.1111/sed.12305

Basalt–seawater interaction, the Plenus Cold Event, enhanced weathering and geochemical change: deconstructing Oceanic Anoxic Event 2 (Cenomanian–Turonian, Late Cretaceous)

HUGH C. JENKYNS*, ALEXANDER J. DICKSON*, MICHA RUHL* and SANDER H. J. M. VAN DEN BOORN†

**Department of Earth Sciences, University of Oxford, South Parks Road, Oxford, OX1 3AN,UK (E-mail: hughj@earth.ox.ac.uk)*

†Shell Global Solutions bv, Kessler Park 1, Rijswijk 2288 GS, The Netherlands

Associate Editor – Ulrich Heimhofer

ABSTRACT

Oceanic Anoxic Event 2 (Cenomanian–Turonian: *ca* 94 Ma) represents a major palaeoceanographic phenomenon that took place during an interval of extreme global warmth when large amounts of organic matter entered the marine burial record, probably triggered by increased availability of nutrients for planktonic biota. Three sections (Eastbourne, Sussex, UK; Raia del Pedale, Campania, Italy; and Tarfaya, Morocco) recording this event illustrate the influence on marine geochemistry of mafic volcanic rock–seawater interaction, anoxia to euxinia, and re-oxygenation and cooling during the so-called 'Plenus Cold Event'. The Eastbourne section represents the organic-lean epicontinental pelagic deposits of the English Chalk; the Raia del Pedale section represents a shallow-water platform carbonate on the Tethyan continental margin, also largely devoid of organic matter; and the Tarfaya core represents an Atlantic margin site where cyclically bedded organic-rich sediments were well developed. Correlation between all three sections is readily achieved by biostratigraphy and carbon-isotope stratigraphy ($\delta^{13}C_{carb}$ and $\delta^{13}C_{org}$) over the Oceanic Anoxic Event 2 interval, represented by a characteristic broad positive carbon-isotope excursion. The stratigraphic range of the Plenus Cold Event, defined by the presence, in two discrete levels, of boreal fauna and an excursion to heavier oxygen-isotope values in the English Chalk, can be identified in Raia del Pedale and Tarfaya by using the carbon-isotope curve as a correlative tool. Similarly, a section in southern France allows its co-existing osmium-isotope excursion to relatively unradiogenic values to be placed in the context of the Oceanic Anoxic Event in all three analysed sections. A fall to lower osmium-isotope values clearly predated the onset of Oceanic Anoxic Event 2, as defined by the initial rise in carbon-isotope values, allowing the putative magmatic/mafic event as a trigger for the Oceanic Anoxic Event. An initial drop in sulphur-isotope ratios ($\delta^{34}S_{CAS}$) at Eastbourne correlates with the osmium-isotope curve, suggesting that isotopically light sulphur could have been derived from a mafic igneous source. Re-oxygenation of sediments of all three investigated sections during the Plenus Cold Event is variably illustrated by change in cerium:calcium, iodine:calcium, molybedenum:calcium and uranium:calcium ratios, according to the redox behaviour of the elements in question and whether controls on seawater chemistry were local or global in nature. Changes in molybdenum-isotope ratios from Tarfaya and portions of the sulphur-isotope curve from Eastbourne and Raia del Pedale also indicate the probable presence of

more oxygen-rich bottom waters during the Plenus Cold Event. Oxidation by such waters of previously deposited organic-rich shales, as well as loss of anoxic/euxinic sinks, is credited with temporarily enriching global seawater in a range of other redox-sensitive trace metals (for example, V, Cr, Co, Ni, Cu, Zn and Cd) during ongoing basalt–seawater interaction indicated by persistent relatively non-radiogenic osmium-isotope seawater values. However, early diagenetic enrichment of manganese in the English Chalk over much of the Oceanic Anoxic Event interval is broadly correlative in time with relatively low osmium-isotope values in sections elsewhere: a relationship that may be due to the lack of affinity of manganese with carbon-rich shales, hence allowing relatively elevated concentrations of the element in marine waters to persist during leaching of mafic rocks, unlike other redox-sensitive species. The calcium-isotope and lithium-isotope ratios from Eastbourne and Raia del Pedale indicate an increase in global weathering during the initial phase of Oceanic Anoxic Event 2, and the shift in strontium isotopes and osmium isotopes to more unradiogenic values during the event suggests that not only construction but also destruction of one or more Large Igneous Provinces was probably a proximal cause of this major palaeoceanographic phenomenon by elevating nutrient levels and planktonic productivity in large tracts of the world ocean. Globally widespread carbon burial and silicate weathering are both identified as important mechanisms for drawing down atmospheric carbon dioxide that, in the absence of overwhelming volcanogenic replenishment of this greenhouse gas during the early phase of Oceanic Anoxic Event 2, caused the Plenus Cold Event.

Keywords Cenomanian–Turonian, Cretaceous, geochemical change, OAE 2, palaeoceanography.

INTRODUCTION

Mesozoic Oceanic Anoxic Events (OAEs) have attracted considerable attention during the last few decades because they illustrate an Earth subject to extreme environmental change, thought to be forced by rapid global warming, probably through the agent of volcanically derived carbon dioxide (Jenkyns, 2003, 2010). Originally recognized by the synchronous or near-synchronous deposition of organic-rich black shales in a global context, the definition and duration of these events can potentially be improved by reference to the global positive carbon-isotope excursion accompanying the massive burial of isotopically light photosynthetically produced planktonic carbon (Schlanger & Jenkyns, 1976; Scholle & Arthur, 1980; Schlanger *et al.*, 1987; Tsikos *et al.*, 2004; Jenkyns, 2010). In some instances, however, isotopically light carbon from sedimentary or volcanic sources has been injected into the ocean–atmosphere system during OAEs, driving carbon-isotope ratios to more negative values and partially overprinting an overarching positive trend (Jenkyns, 2010).

A variety of proxies have been applied in investigations of OAEs to elucidate accompanying geochemical and climatic change, including redox-sensitive isotope systems, organic biomarkers and trace elements. One of the best representatives of Mesozoic OAEs is that of Late Cretaceous Cenomanian–Turonian boundary age (OAE 2: 94 to 93 Ma: Meyers *et al.*, 2012; Ogg & Hinnov, 2012), which was characterized by deposition of organic-rich shales in all ocean basins and many shelf seas (Fig. 1) and accompanied by unambiguous movement of the carbon isotopes in the ocean–atmosphere system to higher values (Schlanger *et al.*, 1987; Hasegawa, 1997; Tsikos *et al.*, 2004; Lenniger *et al.*, 2014). Definition of the duration of OAE 2 is subjective to a degree but is best illustrated by taking the initial level of positive excursion in $\delta^{13}C$ as the onset and the point where a definitive carbon-isotope drop begins as fixing the termination: the suggested duration would hence lie between 400 kyr and 900 kyr (Fig. 2), with the smaller figures potentially

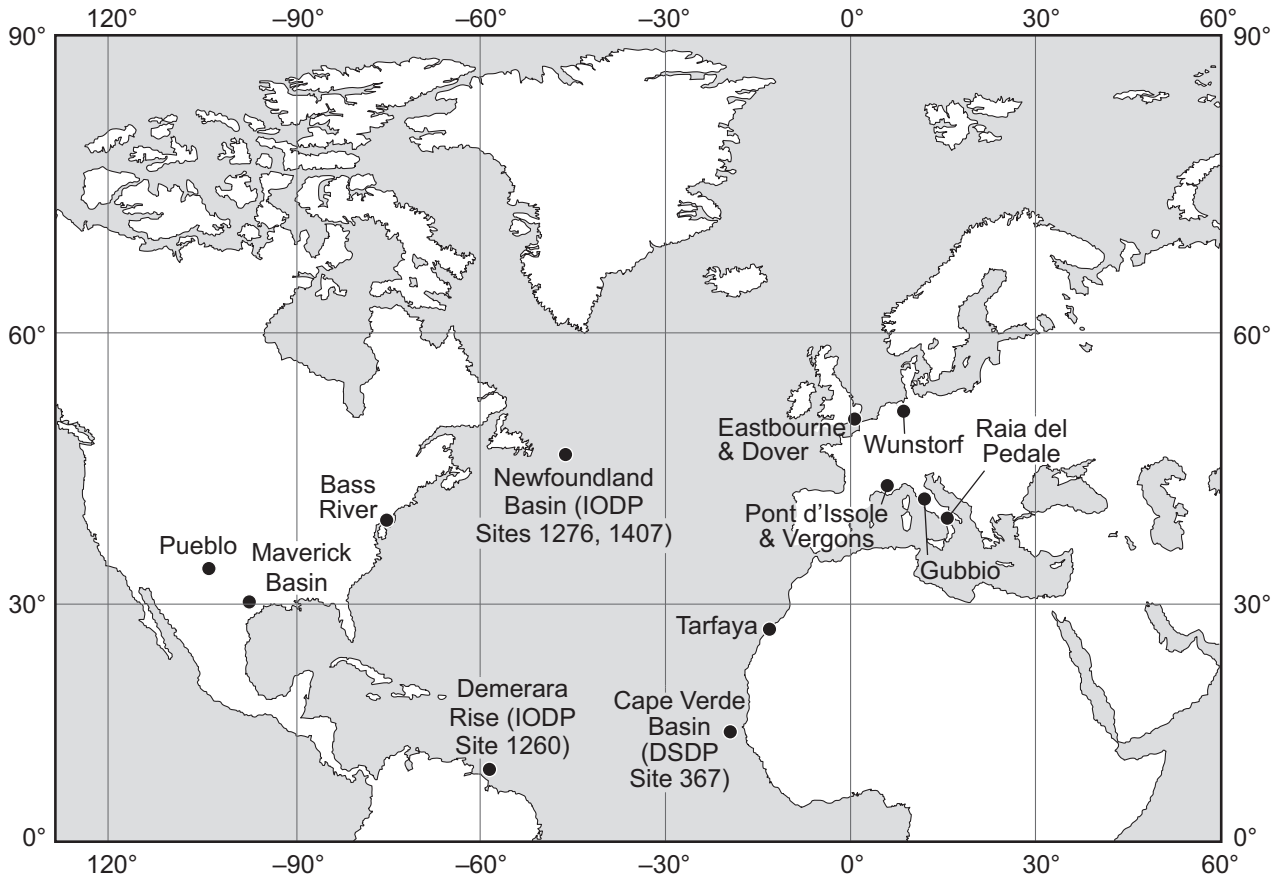

Fig. 1. Principal localities and palaeogeographic entities mentioned in the text where Cenomanian–Turonian boundary sections are situated. Coastal sections at Eastbourne and Dover expose the English Chalk, a pelagic shelf-sea sediment containing nannofossils and planktonic foraminifera as well as a macrofossil biota (Hancock, 1975). Pont d'Issole and Vergons expose a hemipelagic sequence of cyclically bedded limestones and marls with planktonic microfossils and nannofossils (Crumière *et al.*, 1990; Jarvis *et al.*, 2011). Tarfaya represents an unusually organic-rich site, constituted by alternating shales and limestones, sampled from core material (Tsikos *et al.*, 2004). Relevant Atlantic IODP (Integrated Ocean Drilling Program) sites are also illustrated.

compromised by the presence of hiatuses in the sections analysed (Sageman *et al.*, 2006; Voigt *et al.*, 2008; Ma *et al.*, 2014; Eldrett *et al.*, 2015; Gambacorta *et al.*, 2015). Identification of the onset of the positive carbon-isotope excursion is usually unambiguous in $\delta^{13}C$ profiles derived from both carbonate and organic matter but choosing a definitive end-point for the relatively high values can present difficulties. The end-point for the OAE recorded in the Chalk from the Eastbourne section was picked by Tsikos *et al.* (2004) at the Cenomanian–Turonian boundary but subsequent authors have extended it into the lower Turonian (Jarvis *et al.*, 2011; Gambacorta *et al.*, 2015), which is the approach adopted here.

Oxygen-isotope data from benthonic foraminifera from the Atlantic and Pacific oceans, as well as bulk carbonate sediment from the Northern and Southern Hemisphere, suggest that the Cenomanian–Turonian boundary interval recorded extreme global warmth (Jenkyns *et al.*, 1994; Clarke & Jenkyns, 1999; Voigt *et al.*, 2004; Forster *et al.*, 2007a; Friedrich *et al.*, 2012). With particular regard to OAE 2, there is evidence for major geochemical change in the world ocean (Jenkyns, 2010). There is also additional evidence for an accelerated hydrological cycle and increased weathering of silicate rocks during the OAE (Blättler *et al.*, 2011; Pogge von Strandmann *et al.*, 2013).

To date, however, the relative timing and possible cause-and-effect relationships of these disparate phenomena remains poorly defined. Herewith, a range of proxies that have potentially responded to changes in mafic rock–seawater interaction, changes in silicate weathering

intensity and changes in temperature and redox conditions are placed in a high-resolution chemostratigraphic context as defined by carbonate and organic-matter carbon isotopes. The assembled data derive from: (i) the organic-lean English Chalk cropping out in southern England (Eastbourne, Sussex), a pelagic shelf-sea facies rich in nannofossils and planktonic foraminifera; (ii) more organic-rich and clay-rich hemipelagic sections in the Vocontian Trough of south-west France (Pont d'Issole and Vergons); (iii) shallow-water organic-lean [total organic carbon (TOC) generally undetectable except for some rare darker laminites] platform carbonates from Raia del Pedale, Southern Limestone Apennines, Campania, Italy, representing part of the Tethyan continental margin; and (iv) an organic-rich cyclically bedded limestone–mudstone from borehole material at Tarfaya, Morocco, influenced by upwelling on the eastern Atlantic margin (Hancock, 1975; Gale *et al.*, 1993; Tsikos *et al.*, 2004; Kolonic *et al.*, 2005; Parente *et al.*, 2008; Jarvis *et al.*, 2011). The English Chalk in southern England is a particularly valuable archive because of its excellent macrofossil, microfossil and nannofossil biostratigraphy, low organic-carbon values (TOC 0.26% to undetectable), high calcium carbonate content, relative lack of lithification and diagenetic immaturity (Jenkyns *et al.*, 1994). Key outcrop localities are illustrated in Fig. 1, together with other significant OAE 2 sites.

THE PLENUS COLD EVENT DURING OCEANIC ANOXIC EVENT 2

The Plenus Cold Event was first explicitly recognized and named by Gale & Christensen (1996), based on the fossils contained in hemipelagic Upper Cenomanian marls from the Vocontian Trough in south-east France and in coeval epicontinental pelagic chalks in southern England (Fig. 3). The English Chalk contains the belemnite *Praeactinocamax plenus* and associated bivalves (*Oxytoma seminudum*; *Chlamys arlesiensis*) and serpulid worm (*Hamulus* sp.) in the relatively clay-rich Plenus Marls of Late Cenomanian age. The Plenus Marls have been subdivided into Beds numbering 1 to 8 (Jefferies, 1961, 1963 and illustrated in Figs 2 and 3) and the characteristic fauna is most concentrated in Bed 4 but ranges from the top of Bed 3 to Bed 8; *O. seminudum* is also recorded from Bed 2. The absence of these fossils from most of Bed 3 suggests that conditions were not so favourable for the fauna during deposition of this unit.

This unusual faunal assemblage was recognized as having boreal affinities by Jefferies (1961, 1963), based on the occurrence in mid-Cenomanian chalky sediments in the Central Russian faunal province of *Praeactinocamax primus*, thought to be ancestral to *P. plenus* (Fig. 4), as described by Arkhanguelsky (1916). Arkhanguelsky (1916) recognized *Praeactinocamax,* which has a restricted occurrence in the mid-Cenomanian Chalks of southern England, as a species adapted to relatively cool waters, an interpretation now bolstered by oxygen-isotope data on bulk chalks and brachiopod calcite from northern Europe that show movement to heavier values during both the mid-Cenomanian *primus* and Late Cenomanian *plenus* events (Gale & Christensen, 1996; Voigt *et al.*, 2004; Wilmsen *et al.*, 2007). In Chalk sections at both Eastbourne and Dover in southern England, relatively heavy bulk oxygen-isotope values, suggestive of cooling, correlate with the occurrence of *O. seminudum* in Bed 2 of the Plenus Marls; lower $\delta^{18}O$ values characterize Bed 3, implying warming; followed by heavier values in Beds 4 to 8, indicative of renewed cooling (Gale & Christensen, 1996; Figs 2 and 3). Essentially, therefore, both faunal and isotopic data suggest that the Plenus Cold Event was characterized by two cooler water intervals punctuated by an intervening warmer episode. The correlation between cool-water fauna and relatively heavy oxygen-isotope values is clearer at Dover than Eastbourne, suggesting a lesser diagenetic overprint on the chalks exposed at the former locality.

Relatively heavy oxygen-isotope values in examples of *P. plenus* itself, compared with coeval brachiopods from chalks in Germany and England, suggest that the belemnite rostra were secreted in boreal waters and that the organisms were able to migrate southward because mid-latitude waters were cooling (Voigt *et al.*, 2003). *Praeactinocamax* genera hence represent pulse faunas (e.g. Košťák *et al.*, 2004) whose latitudinal distribution was linked to global cooling and/or southerly movement of a boreal water-mass. Rare examples of this genus interpreted as 'northern guests' also occur in the Turonian of Manitoba, Canada, in sediments deposited in the Western Interior Seaway of North America: migration from Siberia has been suggested (Jeletsky, 1950; Košťák & Wiese, 2008). Importantly, however, the Plenus Cold Event occurred during

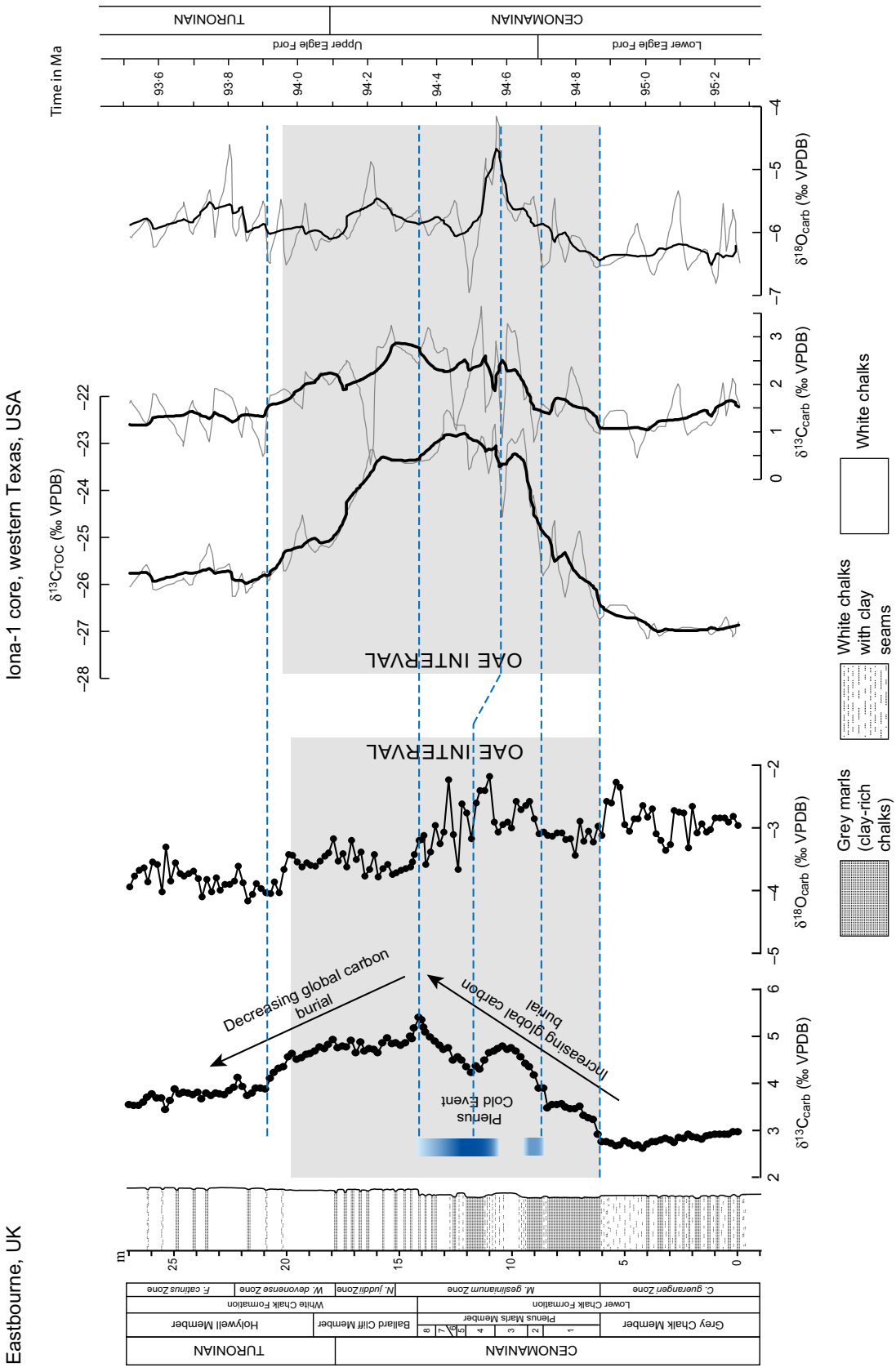
Eastbourne, UK
Iona-1 core, western Texas, USA
CENOMANIAN
TURONIAN
Lower Eagle Ford
Upper Eagle Ford
Time in Ma
93·6
93·8
94·0
94·2
94·4
94·6
94·8
95·0
95·2
Grey Chalk Member
Plenus Marls Member
Lower Chalk Formation
Ballard Cliff Member
Holywell Member
White Chalk Formation
C. guerangeri Zone
M. gestilitanum Zone
N. juddii Zone
W. devonense Zone
F. catinus Zone
m
25
20
15
10
5
0
δ13CTOC (‰ VPDB)
δ13Ccarb (‰ VPDB)
δ18Ocarb (‰ VPDB)
OAE INTERVAL
Plenus Cold Event
Decreasing global carbon burial
Increasing global carbon burial
White chalks
White chalks with clay seams
Grey marls (clay-rich chalks)

Fig. 2. Carbon-isotope and oxygen-isotope stratigraphy of bulk chalks from Eastbourne, Sussex, UK (Tsikos *et al.*, 2004). As in the Dover outcrop (Fig. 3), the Plenus Marls Member is divided into Beds 1 to 8 and correlation of the putative cooler water intervals with relatively heavy bulk oxygen-isotope values is apparent, demonstrating the primary nature of the palaeotemperature signal. Carbon-isotope values show a rising trend over the interval of the Plenus Marls Member and a gently declining trend thereafter, thought to correlate with global patterns of organic-carbon burial. A dip in carbon-isotope values correlates with the Plenus Cold Event, when regionally developed oxygenated bottom waters may have impeded preservation of organic matter on the sea floor, hence lessening preferential extraction of ^{12}C from the ocean–atmosphere system. Based on the carbon-isotope profile, there are two possible picks for the termination level of OAE 2. Rather than taking the pick at the Cenomanian–Turonian boundary (Tsikos *et al.*, 2004), an extension into the lower Turonian is preferred (Jarvis *et al.*, 2006, 2011; Zheng *et al.*, 2013). The Iona-1 record originates from the Maverick Basin, west Texas, USA, and shows variations in $\delta^{13}C_{TOC}$, $\delta^{13}C_{carb}$ and $\delta^{18}O_{carb}$ of the upper and lower Eagle Ford Formation in absolute time and across the Cenomanian–Turonian boundary. The time scale is based on radiometric U/Pb-dating of multiple bentonites within this sequence, combined with cyclostratigraphic and biostratigraphic comparison to Cenomanian–Turonian sequences within the Western Interior Seaway (Eldrett *et al.*, 2015). The light grey line represents the raw data (data-points $<-1‰$ in the $\delta^{13}C_{carb}$ record being omitted), while the thicker black line represents a five-point moving average. Following this correlation sets the duration of OAE 2 as *ca* 900 kyr, which is greater than prior estimates based on study of other sequences that cross the stage boundary but which may contain hiatuses. The OAE interval is shown by the grey band; stratigraphic range of the Plenus Cold Event is shown in blue; horizontal dashed blue line gives suggested correlation, based on the level of initial rise of carbon-isotope values and the biostratigraphically assigned Cenomanian–Turonian boundary. Note the shift to heavier oxygen-isotope values in the base of the Upper Eagle Ford Formation in the Iona Core, probably recording a poorly resolved Plenus Cold Event.

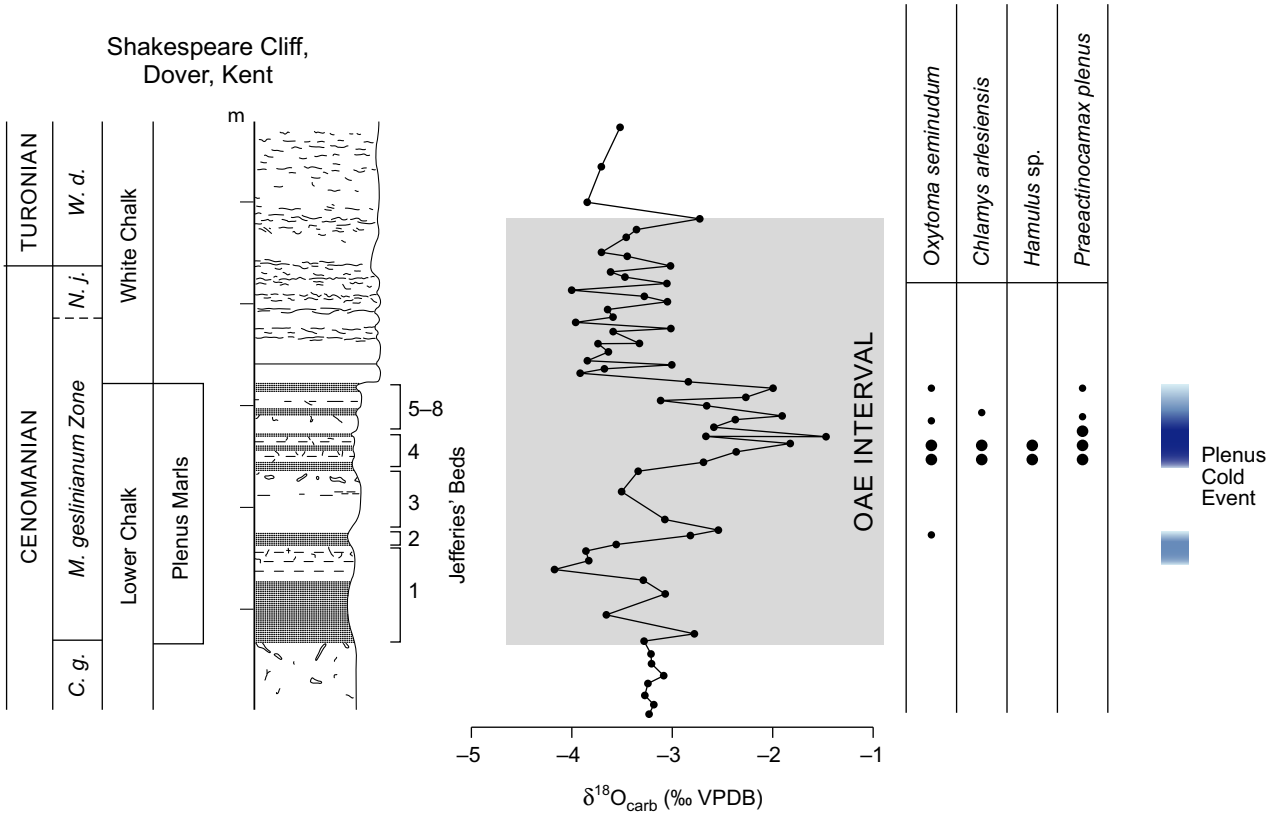

Fig. 3. Oxygen-isotope stratigraphy of the Plenus Marls (Beds 1 to 8) set against the stratigraphic distribution and relative abundance (indicated by the size of the black circles) of the cool-water fauna of the Plenus Cold Event from the Chalk outcrop at Dover, Kent, UK (Gale & Christensen, 1996). Legend as in Fig. 2. Proposed OAE interval is given by the grey band. *Oxytoma* and *Chlamys* are bivalves; *Hamulus* is a serpulid worm; *Praeactinocamax* is a belemnite. The Plenus Cold Event is primarily registered in Beds 4 to 8, although a single faunal element has also been recorded from Bed 2 (Jefferies, 1961, 1963; Gale & Christensen, 1996). Note the correlation of the positive oxygen-isotope values in bulk chalk with the stratigraphic distribution of the cool-water fauna, suggesting that the Plenus Cold Event (shown in blue) can be separated into two separate pulses of reduced seawater temperature: *C. g.* = *C. guerangeri* Zone; *N. j.* = *N. judii* Zone; *W. d.* = *W. devonense* Zone. Oxygen-isotope profile after Lamolda *et al.* (1994).

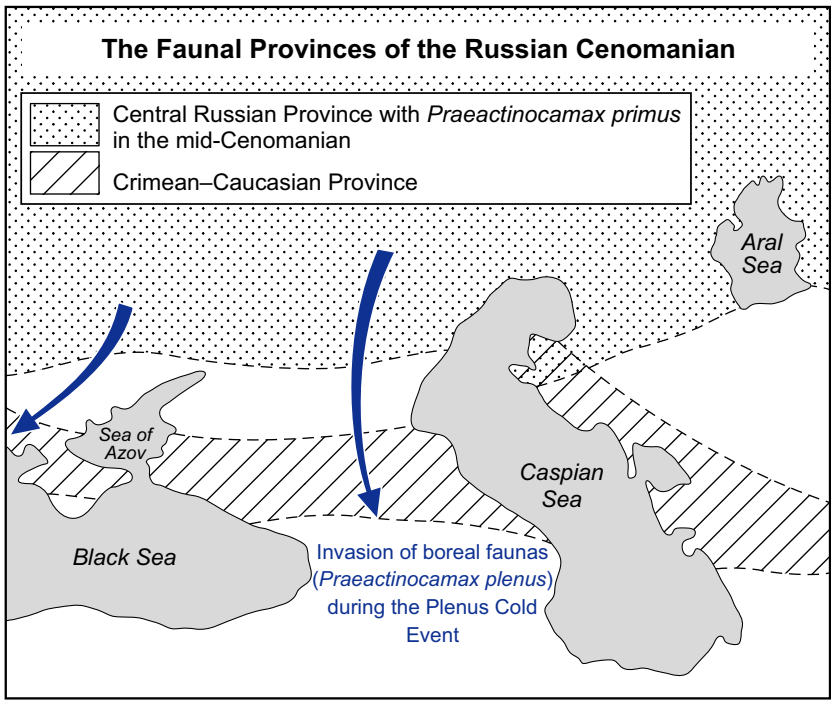

Fig. 4. Faunal provinces of the Russian Cenomanian and postulated southward migration pathways of *Praeactinocamax* genera (belemnites) during the Primus and Plenus Cold Events during the mid-Cenomanian and Late Cenomanian, respectively. After Arkhanguelsky (1916); Jefferies (1961). The interpretation of Arkhanguelsky (1916) of the belemnite fauna as boreal in origin was based on mid-Cenomanian sediments with *Praeactinocamax primus*, younger Cenomanian strata being poorly developed in the Russian area. *Praeactinocamax plenus*, a successor species, was assumed to have occupied similar ecological space to that of *P. primus*. Records of both faunas are present in the English Chalk.

a discrete interval of overall relative global warmth that occurred synchronously with OAE 2 (e.g. Schlanger & Jenkyns, 1976; Schlanger *et al.*, 1987; Jenkyns, 1980, 2003; Arthur *et al.*, 1990; Jenkyns *et al.*, 1994; Hasegawa, 1997; Huber *et al.*, 2002; Norris *et al.*, 2002; Tsikos *et al.*, 2004; Voigt *et al.*, 2004; Sageman *et al.*, 2006; Jarvis *et al.*, 2006, 2011; Forster *et al.*, 2007a,b; Sinninghe Damsté *et al.*, 2010; Friedrich *et al.*, 2012; van Helmond *et al.*, 2013, 2014).

In relatively expanded stratigraphic sequences, the carbon-isotope curve characteristic of OAE 2 possesses enough shape and form to enable it to be used for worldwide correlation not only in pelagic and hemipelagic sequences but also in shallow-water platform carbonates and paralic facies containing plant remains (Gale *et al.*, 1993; Davey & Jenkyns, 1999; Tsikos *et al.*, 2004; Li *et al.*, 2006; Parente *et al.*, 2008; Elrick *et al.*, 2009; Barclay *et al.*, 2010; Jarvis *et al.*, 2011; Joo & Sageman, 2014). Hence, a reference carbon-isotope curve derived from sections containing the fauna of the Plenus Cold Event and diagnostic oxygen-isotope data can be notionally transferred to sections that lack such fossils to aid identification of this key interval or intervals in a variety of sections.

In the Western Interior Seaway of the United States, the relative scarcity of belemnites has not allowed recognition of the event based on the same faunal criteria. However, using carbon-isotope stratigraphy as a correlative tool allows recognition of the same stratigraphic interval, which is characterized by increased abundance of benthonic foraminifera with respect to strata above and below, suggesting improved bottom-water ventilation. This interval of re-oxygenation has been termed the 'Benthonic Zone' or 'Benthic Oxic Zone' (Eicher & Worstell, 1970; Keller & Pardo, 2004; Prokoph *et al.*, 2013; Eldrett *et al.*, 2014), locally contains boreal dinocysts (belonging to the *Cyclonephelium compactum–membraniphorum* morphological plexus) and, by reference to its causative phenomenon, is hereafter ascribed to the 'Benthic Oxic Event'. The event has been recognized in Texas, Colorado (including at Pueblo, the type locality for the base of the Turonian stage: Kennedy *et al.*, 2005), Wyoming, Kansas and South Dakota in the USA, Alberta and Manitoba in Canada but is poorly expressed in some marginal areas (for example, Utah) of the Western Interior Seaway (West *et al.*, 1998; Prokoph *et al.*, 2013; van Helmond *et al.*, 2016). The same event, equally characterized by a relative increase in benthonic foraminifera, has also been recognized in organic-rich sediments from Demerara Rise (Fig. 1) whose Cretaceous palaeoposition was astride the Atlantic Equator (Friedrich *et al.*, 2006) and from Tarfaya, Morocco (Kuhnt *et al.*, 2005; Keller *et al.*, 2008).

The TEX_{86} palaeotemperature data from Atlantic Deep Sea Drilling Project/Integrated Ocean Drilling Program (DSDP/IODP) Sites 367 (Cape Verde Basin) and 1260 (Demerara Rise) suggest a temperature fall of *ca* 4°C during the Plenus Cold Event for the equatorial Atlantic (Forster *et al.*, 2007b) and a larger drop of 5 to 11°C at Site 1276 in the Newfoundland Basin of the North Atlantic (Sinninghe Damsté *et al.*, 2010). Borehole material from Bass River, New Jersey, situated at a roughly comparable palaeolatitude to Site 1276 gave a drop in temperature of *ca* 2·5°C accompanied by invasion of boreal dinocysts in the key interval (van Helmond *et al.*, 2013). A drop of *ca* 5°C was reconstructed for a core from Wunstorf, north Germany (van Helmond *et al.*, 2015). Taken together, the data suggest that cooler oxygenated waters spread southward through the proto-Atlantic and surrounding seas during the first phase of OAE 2. The interval in question can be ascribed to the *Metoicoceras geslinianum* Zone of the Cenomanian Stage in northern Europe, corresponding with the higher levels of the Plenus Marls in the English Chalk (Gale & Christensen, 1996), and to the *Sciponoceras gracile* Zone in the sediments of the Western Interior, corresponding to the lower levels of the Bridge Creek Limestone and the Eagle Ford Formation of the Maverick Basin, west Texas (Elderbak *et al.*, 2014; Eldrett *et al.*, 2014). As far as the record from the Chalk of southern England (Eastbourne) is concerned, the interval characterized by boreal species and relatively heavy oxygen-isotope values correlates with the lower portion of the carbon-isotope curve that defines the OAE 2 interval.

Significantly, the slight dip in the carbon-isotope curve, coincident with the acme of the Plenus Cold Event, may record a temporary drop in the global burial rate of organic matter, as locally recorded by sections in northern Europe (Voigt *et al.*, 2008; Jarvis *et al.*, 2011) and Demerara Rise (Erbacher *et al.*, 2005), implying reduced transfer of photosynthetically produced, relatively ^{12}C-enriched planktonic material into the burial record. Additionally, more O_2-rich bottom waters may have oxidized previously deposited organic matter to return isotopically light carbon to the oceans.

To date, the Plenus Cold Event has only been recognized from outcrops and cores in the Northern Hemisphere, so whether it represents a global cooling or southerly movement of a colder watermass, or both, is not established. However, biomarker evidence from an Atlantic Deep Sea Drilling Project core in the eastern equatorial Atlantic and stomatal indices of fossil leaves from the margins of the Western Interior Seaway suggest a drop in atmospheric CO_2 concentrations during this interval, implying global cooling (Kuypers *et al.*, 1999; Barclay *et al.*, 2010). Similarly, the offset between carbonate and organic carbon isotopes from the d'Issole section, Vocontian Trough, south-east France, implies drawdown of this greenhouse gas over the same period (Jarvis *et al.*, 2011).

Because watermasses during this interval must have contained relatively more oxygen than before and afterwards, a number of geochemical changes in redox-sensitive species should have taken place at different intervals during the OAE. This article examines evidence for such change, with a particular eye for whether local or global effects are recorded. However, other phenomena that may have effected chemical changes in seawater, particularly those that may have confounded the redox signal of OAE 2, also need to be examined.

A MAFIC MAGMATIC 'EVENT' PRECEDING OCEANIC ANOXIC EVENT 2

The osmium-isotope stratigraphy of the OAE 2 interval was first detailed by Turgeon & Creaser (2008) and further amplified by Du Vivier *et al.* (2014, 2015). In all localities investigated, in northern and southern Europe, in DSDP/ODP/IODP North and South Atlantic sites, in mid-continent North America (deposits of the Western Interior Seaway) and in outcrops around the Pacific Rim (Japan and California), isotopic ratios show an abrupt fall to relatively non-radiogenic values whose onset precedes the rise in carbon-isotope values that is conventionally taken to record the onset of the OAE. Given the relatively short residence time of osmium in today's oceans, similar to its mixing time (Peucker-Ehrenbrink & Ravizza, 2000), such an abrupt shift can be interpreted as geologically rapid (<40 kyr) rather than being an artefact of a condensed section or hiatus. In the isotopically well-defined profile from the Vocontian Trough, south-east France (Pont d'Issole & Vergons), osmium-isotope values remain relatively unradiogenic during the stratigraphically lower half of the interval characterized by the relatively high carbon-isotope values before rather abruptly (over an estimated *ca* 80 kyr in terms of time) rebounding

(Du Vivier *et al.*, 2014). Transferring the stratigraphic position of the Plenus Cold Event from Eastbourne (notably, both *P. plenus* and *Hamulus* are recorded from an outcrop in the Vocontian Trough: Gale & Christensen, 1996), using the carbon-isotope curves as a correlative tool, shows relatively low osmium-isotope values before, during and after the cooler interval (Fig. 5), suggesting that magmatic influence, albeit diminishing over time, persisted throughout much of the OAE with no obvious relationship with seawater temperature.

There are other lines of evidence that generally support the coincidence in timing between magmatic influence and the OAE; neodymium-isotope stratigraphy from Demerara Rise (ODP Sites 1256, 1260 and 1261) in the equatorial Atlantic shows a shift to more radiogenic values preceding the OAE, which can be interpreted as registering invasion of a watermass carrying a relatively mafic signature (Martin *et al.*, 2012; Zheng *et al.*, 2013). Evidence for some subaerial volcanic activity comes from the lead-isotope record from the silicate fraction present in the basal levels of the Livello Bonarelli, a black-shale unit in Marche–Umbria, central Italy recording OAE 2 (Kuroda *et al.*, 2007). Whatever the exact mechanism by which the osmium-isotope signature was transferred to global seawater, clear stratigraphic evidence indicates that the shift to non-radiogenic values preceded the rise in carbon-isotope ratios, thus allowing magmatic/mafic influence as a trigger for OAE 2. The time lag between these two geochemical phenomena is estimated as ≤80 kyr (Du Vivier *et al.*, 2015).

ANALYTICAL DATA

The data presented are for a range of geochemical species but, in all cases, they derive from the same sample sets, hence eliminating potential stratigraphic error that could have arisen from conflation of data from different sections or from re-collected material from the same sections. Although the isotopic data derive from published sources, most of the comparisons between the different proxies are made here for the first time. In addition, a range of trace-element/Ca ratios has been newly determined. Solutions for trace-element/Ca ratios from Eastbourne and Raia del Pedale were prepared from 5 mg aliquots of powdered samples of carbonates. Each sample was treated with 2 ml of 0·5 M distilled acetic acid to selectively dissolve carbonates, followed by centrifugation and removal of the supernatant into a second clean centrifuge tube. Solutions were diluted to 10 ppm Ca, and measured using a Thermo Scientific Element 2 magnetic-sector ICP-MS (Thermo Fisher Scientific, Waltham, MA, USA) coupled to an Aridus sample introduction system (Teledyne Cetac, Omaha, NE, USA). Percent accuracy and precision (2 S.D.) of

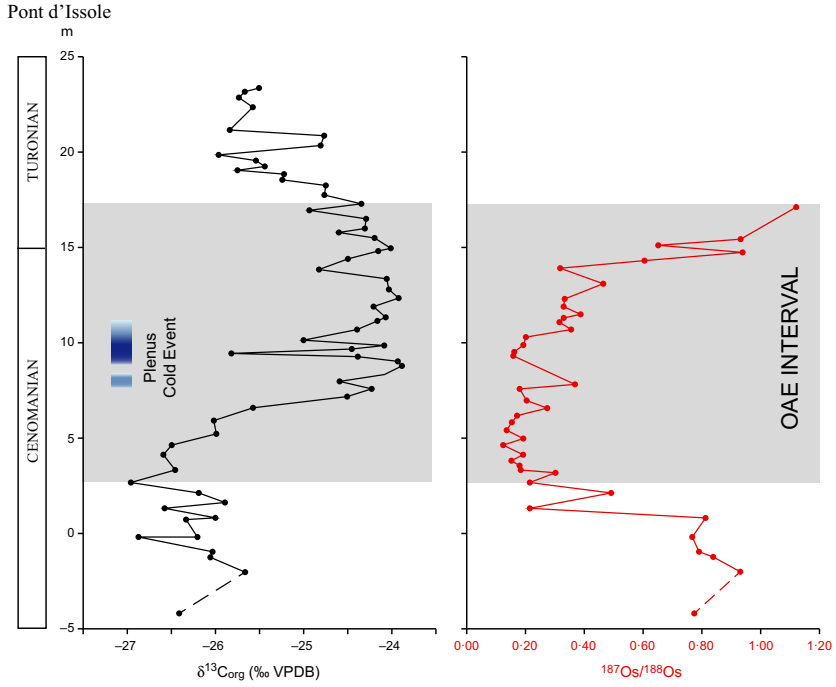

Fig. 5. Carbon-isotope and osmium-isotope profiles from the Vergons and Pont d'Issole sections from the Vocontian Trough, south-east France (Du Vivier *et al.*, 2014), with the stratigraphic position of sediments recording the Plenus Cold Event fixed by reference to the $\delta^{13}C$ profile from Eastbourne (Fig. 2). Interval recording OAE 2 (grey band) is modified from Du Vivier *et al.* (2014) to follow Jarvis *et al.* (2011). The interval of the Plenus Cold Event correlates with relatively low carbon-isotope values but shows no relationship with the osmium-isotope profile. Supply of non-radiogenic osmium from some form of basalt–seawater interaction continued during most of the OAE.

the measured element/Ca ratios were estimated during the run from certified solution standards (n = 14). For Mo/Ca, Cd/Ca, Ce/Ca and U/Ca, precision and accuracy were <4%; for V/Ca, Cr/Ca, Co/Ca, Ni/Ca, Cu/Ca and Zn/Ca, accuracy and precision were <12%; and for Cu/Ca, accuracy and precision were <20%.

As a comparative exercise, Mn/Ca ratios were determined for Eastbourne using the above techniques and compared with the values obtained by Lu *et al.* (2010), illustrated in Fig. 6, who used a stronger acid (3% nitric) to dissolve the calcite in the Chalk. The results were closely comparable in terms of stratigraphic pattern and absolute values, suggesting that loss of metal ions from interaction between clay minerals and acids was minimal in both cases.

COMPARATIVE OCEANIC ANOXIC EVENT 2 CHEMOSTRATIGRAPHY OF CHALKS FROM EASTBOURNE, SUSSEX, UK

Iodine/calcium and manganese/calcium

The I/Ca and Mn/Ca ratios in chalks, illustrated in Fig. 6, show significant excursions over the OAE 2 interval that are best interpreted in terms of redox changes. The iodine/calcium proxy relies on the sensitivity of the dissolved iodate–iodide transition to evolving redox conditions, being one of the first speciation changes to respond to watermass deoxygenation. Importantly, iodate can be incorporated into the calcite lattice, iodide cannot (Lu *et al.*, 2010; Zhou *et al.*, 2015). Substitution of the iodate for the carbonate ion probably takes place primarily in the illuminated upper water column by incorporation into calcareous nannofossils and planktonic foraminifera, so that redox changes in near-surface waters are potentially recorded. The residence time of iodine at the present time is estimated as *ca* 300 kyr (Broecker & Peng, 1982), although the applicability or otherwise of this figure to Cretaceous oceans is unknown.

Overall, the I/Ca ratios at Eastbourne show a step change to higher values correlative with part of the section recording the core of the Plenus Cold Event, implying the development of more oxic near-surface waters from when this event was at its most intense. In more detail, I/Ca ratios begin to rise before any positive movement in the carbon-isotope ratio, then fall back, with some small-scale variation, before beginning their definitive rise. Although the departures from background values are small, surface waters show possible changes in oxygenation in the run-up to, and the onset of, the OAE before becoming definitively and increasingly oxic, continuing into the Turonian under post-OAE conditions. There is, however, no definitive reason why surface and bottom waters should share exactly the same redox pathways and any I/Ca signal will record only local conditions (Zhou *et al.*, 2015).

The relatively elevated content of manganese in the carbonate phase of English and French chalks recording OAE 2 is well documented and is clearly independent of lithology (Schlanger *et al.*, 1987; Jeans *et al.*, 1991; Pratt *et al.*, 1991; Jarvis *et al.*, 2001). Significantly, the data of Pearce *et al.* (2009) show initial movement of Mn values at a lower level in the Eastbourne stratigraphy than the onset of the carbon-isotope shift that conventionally defines the onset of the OAE. These chemostratigraphic relationships are strikingly confirmed by the data of Lu *et al.* (2010), reproduced in Fig. 6, which show relatively elevated levels of manganese that closely parallel the carbon-isotope profile, albeit with the aforementioned offset. The manganese profile is interesting because the vertical extent of the excursion is greater than that of other proxies that show shifts largely confined to the interval covering the stratigraphically lower half of the carbon-isotope excursion.

The short oceanic residence time of manganese (*ca* 1000 years: Broecker & Peng, 1982) is of limited relevance because incorporation of this element into the calcite lattice during early diagenesis requires its reduction to Mn^{2+}, which typically takes place in sediments below the sea floor in a suboxic environment after oxygen and nitrate have been consumed as oxidants of organic matter (Froelich *et al.*, 1979; Berner, 1981). In these circumstances, conditions on the sea floor itself were probably oxic to some degree (Calvert & Pedersen, 1996). Such relatively low-oxygen conditions must have begun to develop before organic-matter burial was significant enough globally to move the global carbon-isotope ratio to more positive values and hence pre-date the OAE, as conventionally defined. Similarly, such conditions, as recorded by some relatively elevated Mn/Ca ratios, persisted when the carbon-isotope curve was on a gentle downward trend and global organic-matter burial rates were declining (Fig. 6).

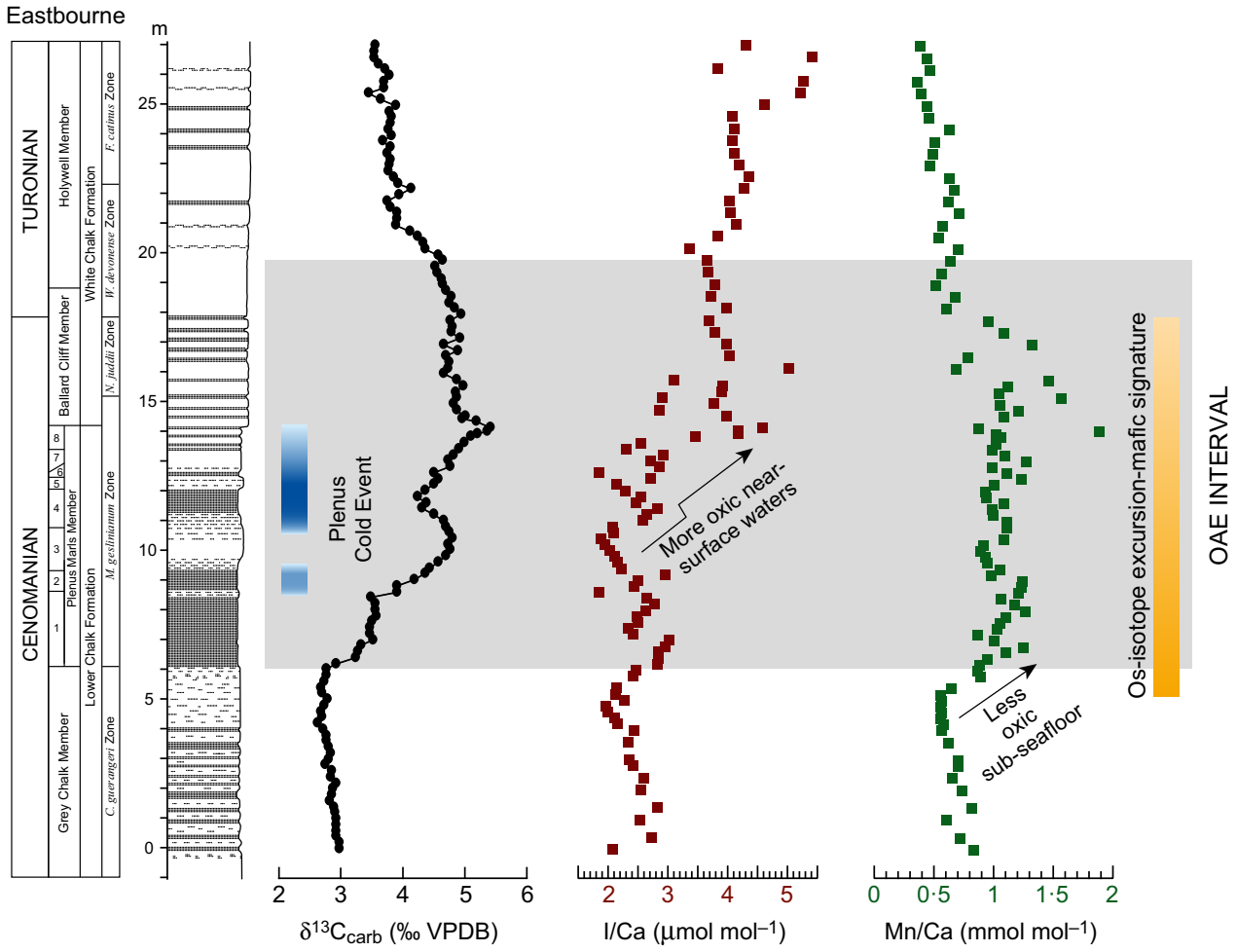

Fig. 6. Iodine/calcium and manganese/calcium ratios from the English Chalk at Eastbourne plotted against the carbon-isotope record, the Plenus Cold Event and the proposed interval affected by the mafic/volcanic/hydrothermal episode illustrated by relatively non-radiogenic osmium-isotope values. Legend as in Fig. 2. Proposed OAE interval is given by the grey band. Relatively low I/Ca values suggest the former presence of the iodide ion in near-surface waters implying deoxygenated near-surface conditions during the initial phase of OAE 2, followed by a step change to more oxic conditions over the interval of the Plenus Cold Event that continued into the Turonian stage. Relatively elevated Mn/Ca ratios over the OAE 2 interval probably record early diagenetic incorporation of the reduced divalent transition metal into carbonates precipitated below the sea floor under dysoxic conditions; correlation with the osmium-isotope stratigraphy is compatible with an igneous source for manganese. Data from Tsikos *et al.* (2004); Lu *et al.* (2010).

Hence, suboxic conditions below the sea floor apparently existed at Eastbourne during most of the OAE and re-oxygenation of bottom waters during the Plenus Cold Event caused little, if any, modification of geochemical processes in sediment pore fluids.

Particularly striking is the correlation between relative manganese enrichment in the Chalk and the proxy osmium-isotope record. Such a correlation leaves open the possibility that the manganese may have had a primary mafic/volcanic/hydrothermal source and was transported as soluble Mn^{2+} across ocean basins from spreading ridges or Large Igneous Provinces (LIPs) through poorly oxygenated waters such as oxygen minima, as originally suggested by Pomerol (1983). Significantly, perhaps, lead isotopes associated with the silicate fraction in an uppermost Cenomanian organic-rich shale from central Italy (the so-called Livello Bonarelli or Bonarelli Level cropping out near Gubbio in Marche–Umbria: Fig. 1) have been proposed as a fingerprint of far-field subaerial volcanism from a LIP (Kuroda *et al.*, 2007).

Manganese is generally not enriched in most organic-rich shales deposited during OAE 2,

probably because of a lack of carbonate alkalinity in the original sediment and/or continued diffusion of a readily reduced element into the overlying water column (Brumsack, 2006; Turgeon & Brumsack, 2006; Jenkyns, 2010; Gavrilov *et al.*, 2013): it would not, therefore, have suffered global depletion in marine waters to the extent potentially experienced by other redox-sensitive elements that could be easily incorporated into sulphides or organic matter.

Cerium/calcium and $\delta^{34}S$

Because cerium, in oxic environments, exists in the tetravalent state, it is efficiently scavenged by hydrous iron-manganese oxyhydroxides in present-day seawater. Seawater, therefore, is characterized by a negative cerium anomaly with respect to other trivalent rare-earth elements, clearly registered in waters from the Atlantic Ocean and waters and fish teeth from the Pacific Ocean, albeit with somewhat different profiles (Goldberg *et al.*, 1963; Elderfield & Greaves, 1982; Wright *et al.*, 1984; German & Elderfield, 1990; Holser, 1997). Although cerium has a very short residence time in present-day oceans (<1500 years: Elderfield & Greaves, 1982; Broecker & Peng, 1982), which would suggest potential strong local geochemical diversity in the abundance of this element in seawater, the widespread presence of oxic sinks at the present time ensures that the negative anomaly is probably a ubiquitous feature in all normal marine environments. In a geological context, negative cerium anomalies are small to non-existent, or even positive, in Lower Palaeozoic and Triassic conodont apatite, corresponding with probable ocean-wide periods of anoxia during which oxyhydroxide sinks for cerium would have been greatly reduced in area and the residence time of the element in seawater greatly enhanced (Wright *et al.*, 1984). With respect to OAEs, chemostratigraphy utilizing the positive cerium anomaly in Lower Cretaceous hemipelagic sediments from the Vocontian Trough has indicated that Tethyan waters were strongly deoxygenated during the early Aptian OAE 1a (Bodin *et al.*, 2013). Given the global spread of Lower Aptian organic-rich shales (Arthur *et al.*, 1990; Bralower *et al.*, 1994), the positive cerium anomaly is likely to have been a global feature but differ in aspect from place to place. A positive cerium anomaly is also illustrated in pelagic non-bioturbated nannofossil chalks and clays from a core crossing the Cenomanian–Turonian boundary taken by the Ocean Drilling Program (ODP Site 762 off western Australia) and interpreted as resulting from the loss of Fe-Mn oxyhydroxide sinks either locally or globally (Dickens & Owen, 1995).

The Eastbourne profile (Fig. 7) shows a clear overall positive shift in Ce/Ca, with the onset of higher values beginning below the level where carbon isotopes start to rise, thus recording local or regional changes to less oxygenated conditions before the onset of the OAE, as conventionally designated (Lu *et al.*, 2010). Significantly, elevated nannofossil and dinocyst fertility indices are present in this pre-OAE interval, suggesting increased organic carbon flux through the water column, probably driving deoxygenation (Pearce *et al.*, 2009). Shifts to more local or regional oxic conditions are recorded in Bed 2 and the lower part of Bed 3 of the Plenus Marls by a dip in Ce/Ca values and show partial correlation with the early cool pulse of the Plenus Cold Event (Fig. 7). Higher levels in the section, around Bed 4 of the Plenus Marls, show another positive shift, before values fall again, corresponding with the core level of the Plenus Cold Event. The fact that the inferred changes in redox correlate only partially with the Plenus Cold Event and its precursor suggests some degree of local control on sea-floor oxygenation and availability of potential Fe–Mn oxyhydroxide sinks for cerium. The overarching positive Ce/Ca anomaly finishes with a return to background where the Plenus Marls pass into overlying chalks (Bed 8), in correspondence with the stratigraphic level where the highest carbon-isotope values are attained. Higher in the section, Ce/Ca values gently decline to background levels similar to those registered below the strata that record the OAE. It is notable that the overarching positive cerium anomaly occurs only in the sediments whose carbon-isotope ratios record the first half of the OAE, embracing the entire Plenus Marls and *ca* 1·5 m of sediments below this unit.

Sulphur isotopes ($\delta^{34}S_{CAS}$) also have the potential to record redox changes in the oceans, and because the present-day residence time of sulphate is measured in millions of years (13 to 20 Myr), the isotopic signature is effectively homogenous (e.g. Bottrell & Newton, 2006). Hence, on the assumption that the oceanic sulphate residence time was not an order of magnitude lower than this figure during the Late Cretaceous (sulphate concentrations in Cenomanian seawater are estimated as only about half that of the present day: Timofeeff *et al.*, 2006),

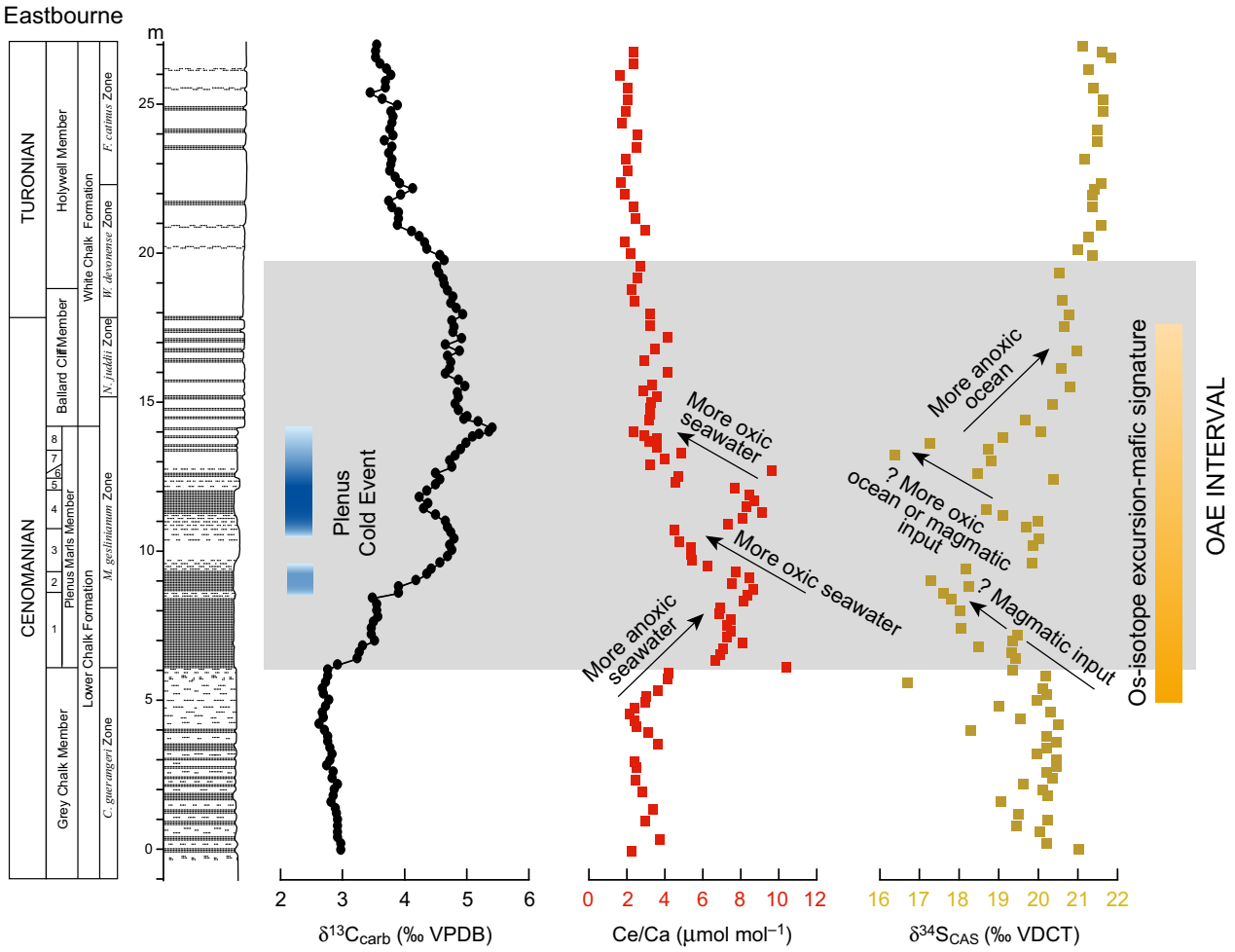

Fig. 7. Cerium/calcium and $\delta^{34}S$ of carbonate-associated sulphate from the English Chalk at Eastbourne plotted against the carbon-isotope record, the Plenus Cold Event and the proposed interval affected by the mafic/volcanic/hydrothermal episode. Legend as in Fig. 2. Proposed OAE interval is given by the grey band. Higher Ce/Ca ratios indicate a reduction in local oxy-hydroxide sinks for cerium, so that the overarching positive excursion records the first half of the OAE up to the level of peak carbon-isotope values. Shifts to lower Ce/Ca show some correlation with the two phases of the Plenus Cold Event, although the final shift to lower values essentially constitutes a step change, with values indicating generally more oxic conditions locally, even though carbon-isotope values recording the global signal remain relatively high. $\delta^{34}S$ values, probably reflecting global seawater, show a shift to lower values at a stratigraphic level below the onset level of the OAE and well below the level of the Plenus Cold Event but commensurate with the position of osmium-isotope shift to less radiogenic values. Volcanic/hydrothermal input of isotopically light sulphur is hence a possibility. Higher in the section, $\delta^{34}S$ recovers somewhat before dropping to lower values that could record oxidation of previously deposited pyrite in globally distributed organic-rich sediments and consequent release of isotopically light sulphur during the Plenus Cold Event. These effects may have kept sulphur-isotope values relatively low during the early phase of the Oceanic Anoxic Event, although maximum post-OAE $\delta^{34}S$ values may also reflect the greater residence time of sulphate over dissolved inorganic carbon in the world ocean. Data from Tsikos *et al.* (2004), Lu *et al.* (2010), Owens *et al.* (2013).

the sulphur-isotope stratigraphy, if unmodified by diagenesis, of any one section should reflect that of the world ocean. The major factor controlling the $\delta^{34}S$ composition of seawater is the amount of reduced sulphur buried as part of organic matter and pyrite, because of the strong preference for the lighter isotope during bacterial sulphate reduction within the water column and below the sea floor. Hence, during OAEs characterized by widespread anoxic to euxinic environments, the sulphur-isotope composition of seawater should increase concomitantly with the burial of reduced sulphur compounds. Such has proven to be the case for

OAE 2 (Ohkouchi *et al.*, 1999; Owens *et al.*, 2013; Gomes *et al.*, 2016) although, notably, peak sulphur-isotope values occur stratigraphically higher than do peak carbon-isotope values in all investigated European sections.

The Eastbourne section offers a chance to examine the high-resolution sulphur-isotope evolution of the world ocean utilizing carbonate-associated sulphate (Owens *et al.*, 2013). As with the Ce/Ca ratio, significant geochemical change occurs in levels recording the initial half of the OAE, although $\delta^{34}S$ continues to rise to the top of the section, whereas carbon isotopes at this stratigraphic level have relaxed to near-background values (Fig. 7). The offset between maximum sulphur-isotope and maximum carbon-isotope values was attributed by Owens *et al.* (2013) to the greater residence time of sulphate compared with that of dissolved inorganic carbon, allowing $\delta^{13}C$ to return to background values more rapidly. However, detailed inspection of the Eastbourne geochemical profiles suggests that other mechanisms may have been responsible for keeping sulphur isotopes at relatively low values during the early OAE interval. Although $\delta^{34}S$ values show a certain amount of scatter, a definitive shift to lower values takes place in the lower part of the section beginning close to the level of the initial rise in carbon isotopes, clearly below the level that records the Plenus Cold Event. Hence, the drop in sulphur-isotope ratios cannot be due to oxidation of significant quantities of previously precipitated pyrite because anoxic conditions were becoming globally more significant at this time. Significantly, however, the negative shift in $\delta^{34}S$ correlates closely in time with the seawater $^{187}Os/^{188}Os$ shift to lower values (Fig. 6), implying a possible relationship with the causal factors, such as volcanism, hydrothermal activity, creation and destruction of a LIP, that lie behind the mafic osmium-isotope signature. Volcanism and hydrothermal activity are documented sources of isotopically depleted sulphate (δ^{34} S = 0 to 3‰ but very variable) to the present-day world ocean (Holser & Kaplan, 1966; Walker, 1986; Paytan *et al.*, 2004; Bottrell & Newton, 2006).

Such a relationship has been suggested for OAE 2 based on carbonate sulphur-isotope data from Colorado, USA, deposited in the Western Interior Seaway of North America and sections in Italy and France (Pont d'Issole), but modelling suggests the proviso that the world ocean must have been more depleted in sulphate at this time than it is today (Adams *et al.*, 2010; Gomes *et al.*, 2016). Addition of sulphate from mafic-rock–seawater interaction may have increased global pyrite formation at the expense of iron oxyhydroxides, hence removing a sink for dissolved phosphate and allowing more of it to remain in seawater to fuel organic productivity and help drive the OAE (Gomes *et al.*, 2016).

The negative $\delta^{34}S$ excursion is followed up-section in European sections by movement to more positive values, suggesting that sinks for reduced sulphur compounds became relatively more important as the OAE took hold, before another negative shift is developed, correlating closely with the level of the Plenus Cold Event. This latter negative $\delta^{34}S$ shift can thus be interpreted as due to regional to global re-oxygenation of the shallow sub-sea floor and oxidation of pyrite and other reduced sulphur compounds, introducing preferentially ^{32}S-rich sulphate into ocean waters. However, a source from mafic rock–seawater interaction cannot be excluded, as reference to the osmium-isotope curve suggests that such phenomena were also ongoing at this time. Higher in the section, extending into the post-OAE interval, the marine sulphur-isotope signature was dominated by global fixation of isotopically light sulphur compounds, rendering seawater increasingly isotopically heavy, even when dissolved inorganic carbon had relaxed towards background isotopic values (Owens *et al.*, 2013).

Chromium and Vanadium

The Cr/Ca ratios and V/Ca ratios, illustrated in Fig. 8, show clear positive excursions at the stratigraphic level of the Plenus Cold Event. Similar profiles are exhibited by a broad range of redox-sensitive metals (V, Cr, Co, Ni, Cu, Zn and Cd) and remain when the metal concentrations are normalized against Al or Zr to eliminate possible bias due to stratigraphic changes in the clay/calcite ratios in the Chalk. This phenomenon was first recorded by Orth *et al.* (1993), not only from Eastbourne but also from Upper Cenomanian strata in many other parts of the world. Pearce *et al.* (2009) noted a rise in Cr/Al ratios in the Plenus Marls at Eastbourne beginning in Bed 4 and reaching a maximum in Bed 6, a pattern that conforms to that displayed here and is manifestly independent of lithology (Fig. 8). Significantly, Bed 4 contains the greatest density of boreal species and chalks with the heaviest oxygen-isotope values, suggesting deposition in the coldest and therefore most

oxygenated waters (Fig. 3). Trace-element 'spikes', similarly normalized against Zr and Al to eliminate bias from terrestrially derived material, and set against high-resolution carbon-isotope curves, are documented from Upper Cenomanian sediments deposited in the Western Interior Seaway of North America and from a platform carbonate in southern Mexico; these intervals of relative metal enrichment manifestly correlate in time with the Plenus Cold Event/Benthic Oxic Event (cf. Snow *et al.*, 2005; Elrick *et al.*, 2009; Eldrett *et al.*, 2014).

Although these elevated trace-element levels have been conventionally interpreted as recording volcanism, or at least some kind of mafic rock–seawater interaction somewhere in the world ocean, as also supported by chromium-isotope data from the Western Interior Seaway (Holmden *et al.*, 2016), there are problems with this interpretation. Specifically, there is no consistently developed trace-element 'spike' or step change (apart from Mn: Fig. 6) at the level of osmium-isotope shift to less radiogenic values (Fig. 8), as would be predicted if reaction between seawater and basaltic rocks had flooded the ocean with metal ions whose residence time was probably some thousands or tens of thousands of years (Broecker & Peng, 1982). It, thus, seems more probable that during the Plenus Cold Event, while basalt–seawater interaction continued to be important as indicated by the global osmium-isotope signature, the sinks for such trace elements were much reduced and oxidation of previously deposited organic-rich shales and accompanying sulphides (that characterized the early phase of the OAE) also took place, liberating metals previously

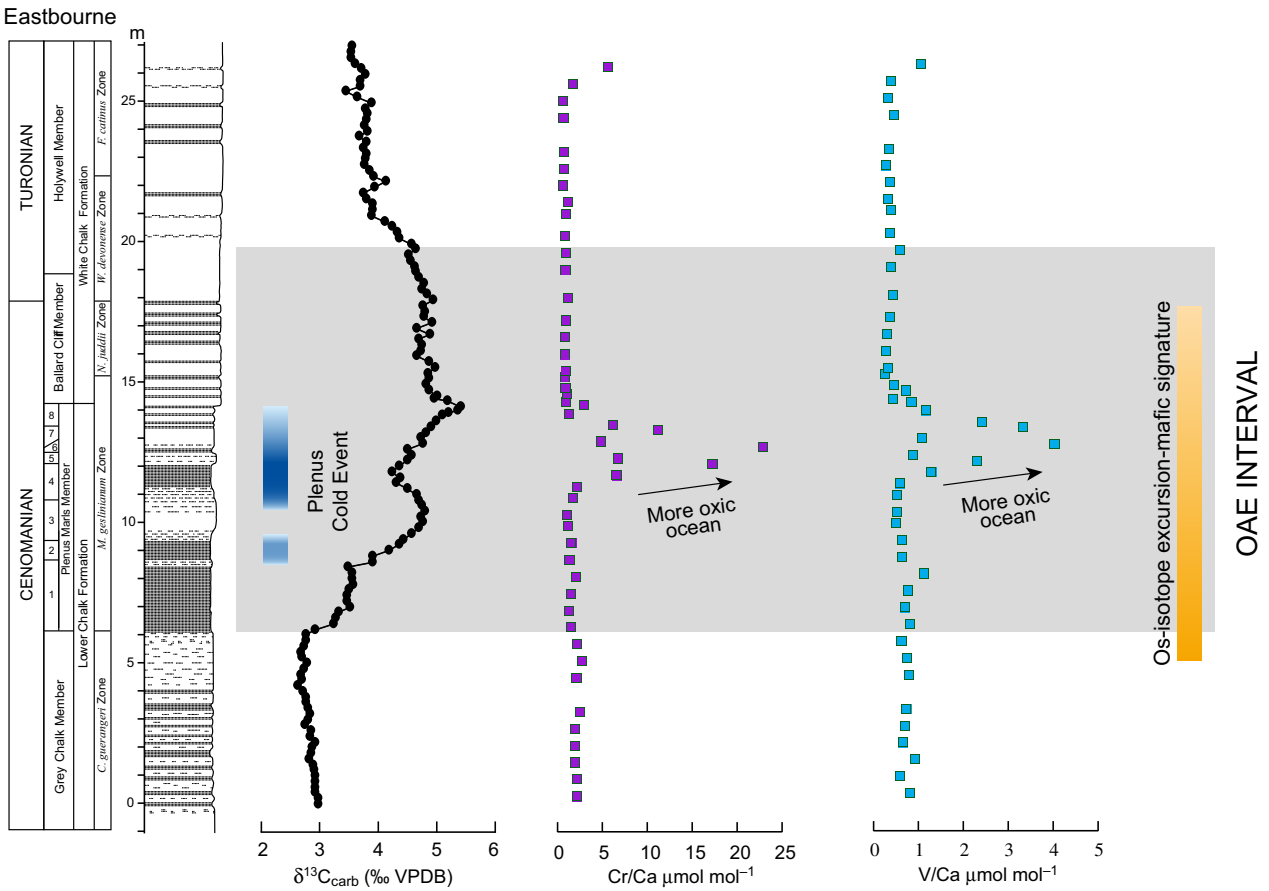

Fig. 8. Chromium/calcium and vanadium/calcium ratios from the English Chalk at Eastbourne plotted against the carbon-isotope record, the Plenus Cold Event and the proposed interval affected by the mafic/volcanic/hydrothermal episode. Legend as in Fig. 2. Proposed OAE interval is given by the grey band. The trace-element 'spike' in Cr and V correlates with the interval of the Plenus Cold Event, during which the global area of anoxic sinks for redox-sensitive species would have been reduced and oxidation of previously deposited organic matter and pyrite could have liberated many metal elements. Ongoing basalt–seawater interaction would also have introduced metal ions that potentially remained in seawater at this time.

adsorbed onto organic matter and pyrite. Redox-sensitive trace metals are known to be relatively concentrated in organic-rich shales deposited during OAE 2, although this enrichment needs to be viewed in the context of global drawdown under regionally extensive anoxic to euxinic conditions that led to drops in relative abundance in any one section (Arthur *et al.*, 1990; Brumsack, 2006; van Bentum *et al.*, 2009; Hetzel *et al.*, 2009; Gavrilov *et al.*, 2013; Goldberg *et al.*, 2016; Dickson *et al.*, 2017).

The phenomenon of trace-metal liberation is in agreement with the negative shift in seawater sulphur-isotope values, probably due to globally significant oxidation of pyrite, which correlates with the level of the Plenus Cold Event seen at Eastbourne (Fig. 7). Although metals must have been supplied to the world ocean from mafic rock–seawater interaction at a relatively elevated rate beginning at a time indicated by the negative osmium-isotope shift, contemporaneous accelerated deposition of organic-rich sediments as the OAE began to take hold would have kept their concentrations relatively low until a change in redox conditions allowed their release. A clear exception to this rule is manganese (Fig. 6) that shows increases correlating with the onset of the osmium-isotope excursion, pre-dating the OAE level, and continued relative enrichment that closely parallels the entire positive carbon-isotope excursion.

In summary, during the early phase of OAE 2, organic-rich sediments could have acted as a geochemical capacitor for a wide range of redox-sensitive metals that were released during the regional bottom-water oxygenation characterizing the Plenus Cold Event, at which time supply of such metals to the world ocean from ongoing basalt–seawater interaction must also have taken place.

Trace-metal 'spikes' are also recorded from a number of sections in Europe and the Pacific Ocean that record the early Aptian OAE 1a, although this event is remarkably complex in detail. Notably, the highest values of these elements are observed in sediments deposited under the least strongly oxygen-depleted conditions (Erba *et al.*, 2015).

δ^7Li and $\delta^{44/42}$Ca

Calcium isotopes and lithium isotopes, which are isotopically homogenous in present-day seawater due to their relatively long residence time (*ca* 10^6 years), constitute isotopic proxies that potentially respond to silicate weathering. Although the available data are relatively low resolution, both geochemical species show excursions to lower values in the Eastbourne section (Blättler *et al.*, 2011; Pogge von Strandmann *et al.*, 2013). With respect to calcium, the isotopic profile shows a general drift to lower $\delta^{44/42}$Ca values in the lower half of the section terminating at a level close to the half-way mark of the OAE interval, as defined by the carbon-isotope curve, and then stages a recovery up-section (Fig. 9). There is no straightforward relationship with the Plenus Cold Event although, as with most other geochemical species, the recovery towards higher (background) values in $\delta^{44/42}$Ca begins well below the termination level of the OAE, and there is something of a step change in the record beginning at the level of the Plenus Cold Event.

The onset of the negative lithium-isotope excursion begins at a lower position in the stratigraphy than that displaying the initial rise in carbon isotopes and has effectively recovered by the midpoint of the OAE level (Fig. 9). However, the initiation level of the negative δ^7Li excursion correlates with the onset of the osmium-isotope excursion to less radiogenic values. Hence, rather than simple increased weathering of continental rocks during the OAE under the influence of an accelerated hydrological cycle, submarine and subaerial processes involving alteration of mafic minerals during construction and destruction of LIPs are equally compatible with the geochemical data. Large igneous provinces potentially involved in the genesis of OAE 2, include the Arctic, Caribbean and Ontong Java Plateaus and the Madagascar Flood Basalts, and their extrusion was probably accompanied by accelerated global seafloor spreading rates (Sinton & Duncan, 1997; Kerr, 1998; Jones & Jenkyns, 2001; Courtillot & Renne, 2003; Barclay *et al.*, 2010; Jarvis *et al.*, 2011; Zheng *et al.*, 2013, 2016). Both submarine and subaerial extrusion of basaltic material has been suggested (Kuroda *et al.*, 2007). Neodymium-isotope ratios from fish teeth extracted from the Chalk at Eastbourne point particularly to the Arctic as a significant source of basalt-derived metals during the Plenus Cold Event (Zheng *et al.*, 2013).

Higher in the section, a possible decrease in weathering can be seen in the lithium-isotope record, broadly correlative with the Plenus Cold Event, which could be interpreted as reduced reaction between water and silicate minerals under cooler climatic conditions: such effects would presumably have been more significant if by this time formerly submarine LIPs had become emergent. If these δ^7Li data do indeed record this

switch in weathering rates, the residence time of lithium in the oceans may have been less than the *ca* 1·2 million years it is at the present day (Misra & Froelich, 2012), given the assumed duration (400 to 900 kyr) of the OAE (e.g. Sageman *et al.*, 2006; Voigt *et al.*, 2008; Ma *et al.*, 2014; Eldrett *et al.*, 2015).

COMPARATIVE OCEANIC ANOXIC EVENT 2 CHEMOSTRATIGRAPHY OF PLATFORM CARBONATES FROM RAIA DEL PEDALE, CAMPANIA, ITALY

Cerium/Calcium and $\delta^{34}S$

The Raia del Pedale section, with the inferred stratigraphic position of the level recording the Plenus Cold Event and, similarly, the osmium-isotope excursion, is illustrated in Fig. 10. The Ce/Ca ratios show a well-defined and coherent negative excursion in the lowest part of the section reaching a minimum at a position corresponding to the core of the Plenus Cold Event before recovering to higher and more scattered values. Given the shallow-water nature of the deposit, which contains abundant benthonic fauna such as rudists and foraminifera, local oxic sinks for cerium are likely to have been present, probably enhanced by increased oxygenation during the Plenus Cold Event. Local removal of dissolved cerium during the early part of the OAE may, therefore, have taken place. However, the rise in Ce/Ca values higher in the section, corresponding with the latter part of the OAE interval, suggests that the sediments may be recording

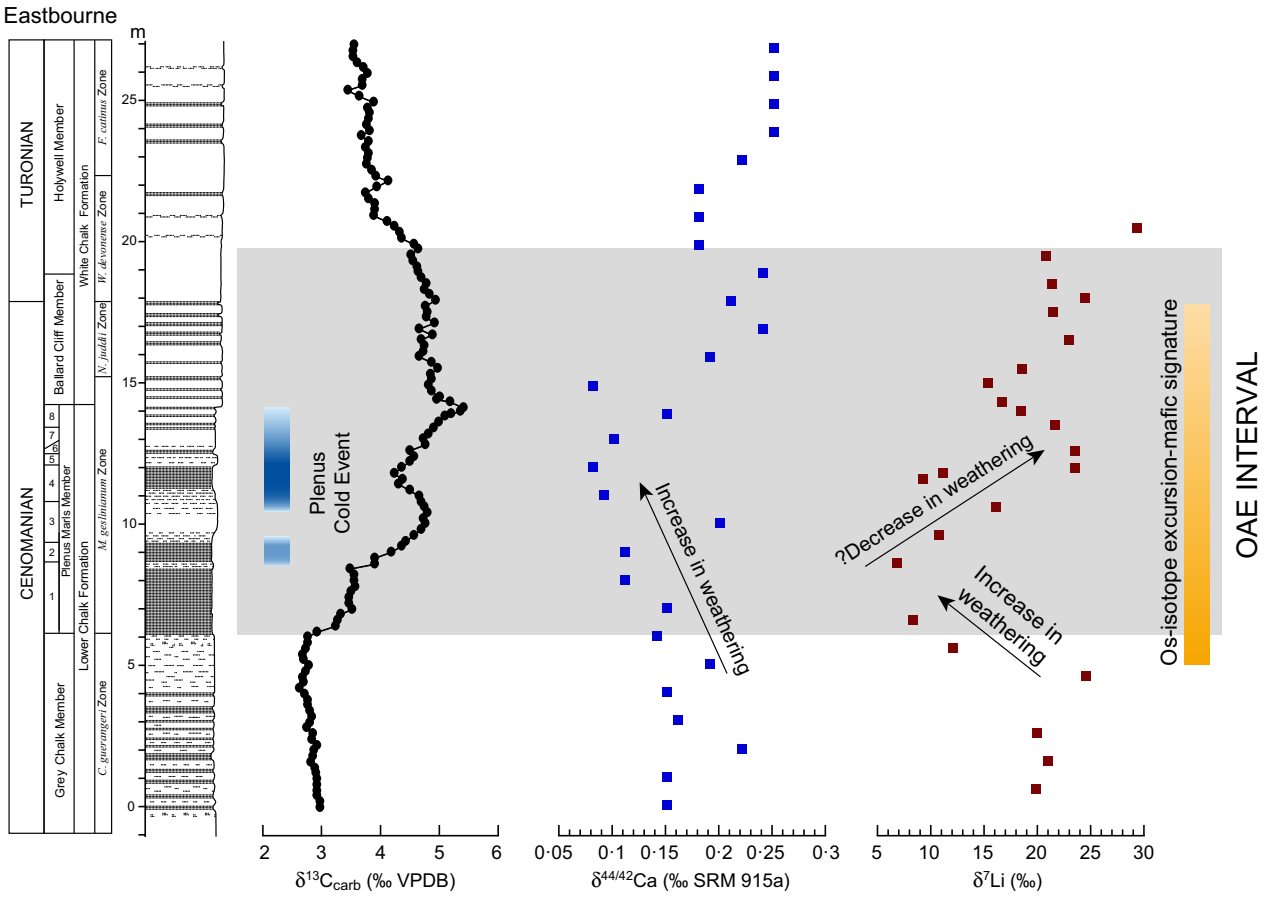

Fig. 9. Calcium isotopes and lithium isotopes from the English Chalk at Eastbourne plotted against the carbon-isotope record, the Plenus Cold Event and the proposed interval affected by the mafic/volcanic/hydrothermal episode. Legend as in Fig. 2. Proposed OAE interval is given by the grey band. There is a broad negative excursion in calcium isotopes over the initial half of the OAE, interpreted as due to increased weathering. Lithium isotopes show more detailed trends, indicating an initial shift at the level of the onset of the osmium-isotope excursion, possibly pointing to weathering of subaqueous or subaerial mafic material, followed by a possible decrease over the interval of the Plenus Cold Event when the cooler climates would have reduced degradation of silicate minerals. Data from Tsikos *et al.* (2004); Blättler *et al.* (2011); Pogge von Strandmann *et al.* (2013).

global increase in dissolved seawater cerium, reflecting increasingly important effects from the spread of anoxic environments and consequent loss of regionally extensive oxic sinks. It is notable that the Ce/Ca ratios in the platform carbonates are an order of magnitude less than those in the chalks from Eastbourne, which underscores the local control on this geochemical proxy.

The sulphur-isotope signature of the Raia del Pedale section shows more scatter than does Eastbourne, but the underlying trend is similar (Owens *et al.*, 2013). The shift to lower $\delta^{34}S$ values at the base of the section is poorly defined but covers the interval where osmium isotopes show an abrupt fall to less radiogenic values as well as the interval corresponding to the Plenus Cold Event. Unlike Eastbourne, recognition of two distinct negative sulphur-isotope shifts is not possible, but the data are compatible both with phenomena such as volcanism, hydrothermal activity, creation and destruction of a LIP, and regional re-oxidation of isotopically light reduced sulphur compounds. As with Eastbourne, maximum sulphur-isotope values are achieved above the OAE interval where carbon-isotope values have declined to background levels, interpreted

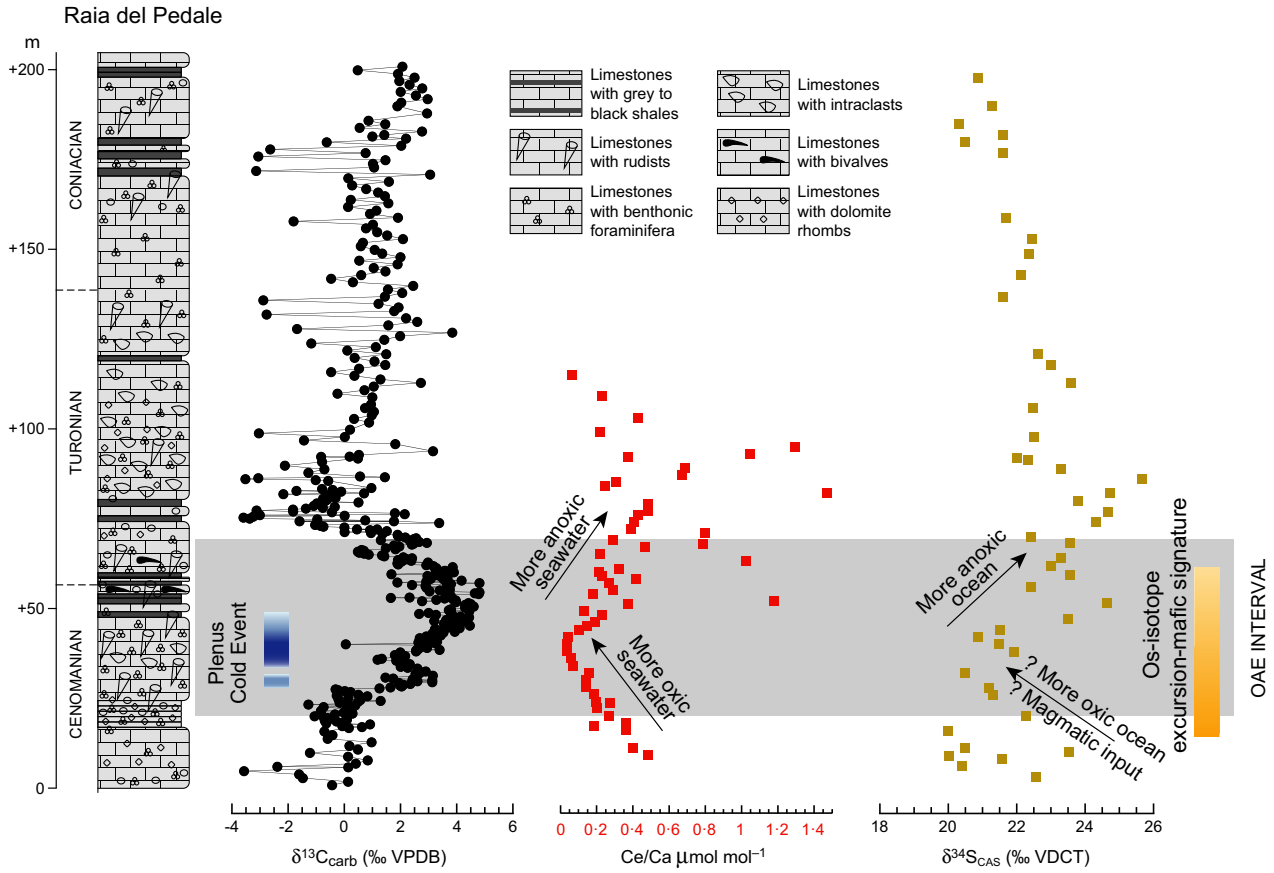

Fig. 10. Ce/Ca and $\delta^{34}S$ of platform carbonates from Raia del Pedale, Campania, Italy, plotted against the carbon-isotope record and the proposed intervals affected by the Plenus Cold Event and the mafic/volcanic/hydrothermal episode illustrated by relatively non-radiogenic osmium-isotope values. Ce/Ca shows a dominant shift to lower values including over the interval of the Plenus Cold Event, followed by a positive trend, albeit with more scattered values. Higher values probably reflect regional loss of oxic sinks for this rare-earth element. The general negative shift in $\delta^{34}S$ at the base of the section correlates with the onset of the osmium-isotope excursion but also overlaps with the level of the Plenus Cold Event, so separation of these two phenomena that could have introduced isotopically light sulphur into the ocean is not possible, as it is in Eastbourne. Higher in the stratigraphy, the sulphur-isotope values show a pronounced positive trend taken to record global seawater under the influence of massive pyrite precipitation during the OAE. Post-OAE peak $\delta^{34}S$ values can be attributed to the greater residence time of sulphate over dissolved inorganic carbon in the world ocean as well as the factors introducing isotopically light sulphur to the oceans during the early stages of the Oceanic Anoxic Event. Data from Owens *et al.* (2013) and the present study.

as a response to the shorter residence time of the inorganic-carbon relative to the sulphate reservoir (Owens *et al.*, 2013). The differences between the Raia del Pedale profile and that of Eastbourne, with the former showing larger magnitude excursions in sulphur-isotope ratios, may reflect regional variation in isotopic composition of seawater from a relatively low sulphate ocean, for which there is independent evidence from fluid inclusions in marine halite (Timofeeff *et al.*, 2006; Owens *et al.*, 2013).

$^{87}Sr/^{86}Sr$ and $\delta^{7}Li$

Bulk strontium-isotope ratios of platform carbonates from Raia del Pedale (Fig. 11), although showing some degree of scatter (Owens *et al.*, 2013; Pogge von Strandmann *et al.*, 2013), illustrate a distinct trend that conforms to established global patterns by showing general evolution towards less radiogenic values beginning in the Late Cenomanian and extending into higher stages of the Cretaceous (McArthur *et al.*, 1993, 1994; Bralower *et al.*, 1997; Jones & Jenkyns, 2001; Ando *et al.*, 2009). However, ultra-high-resolution strontium-isotope analysis of rudist bivalve fragments from a Cenomanian–Turonian shallow-water section elsewhere in southern Italy has revealed a brief excursion to more radiogenic values over the interval characterized by the initial rise in carbon-isotope values and, hence, apparently just pre-dating the onset of the Plenus Cold Event (Frijia & Parente, 2008; Jenkyns, 2010). This transient increase in $^{87}Sr/^{86}Sr$ suggests that continental weathering briefly assumed greater relative importance than

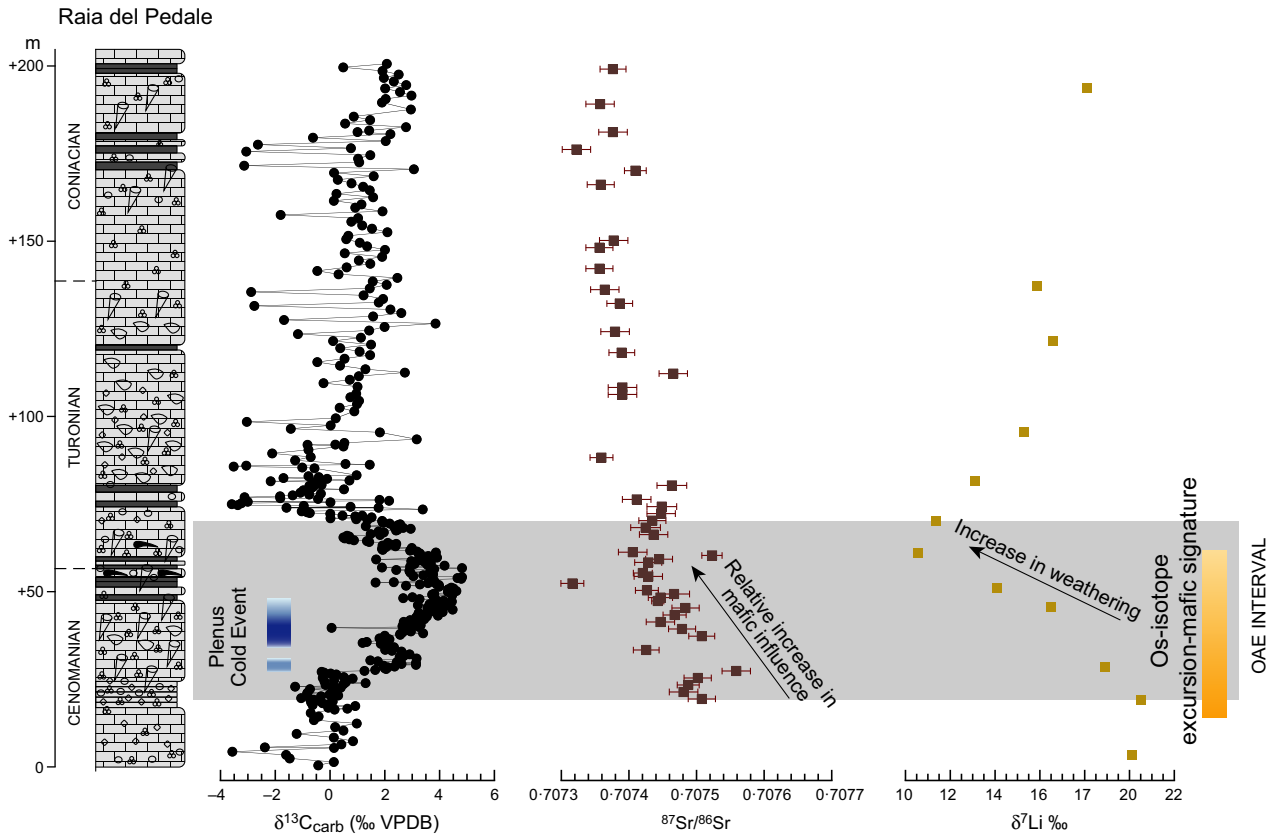

Fig. 11. $^{87}Sr/^{86}Sr$ and $\delta^{7}Li$ of platform carbonates from Raia del Pedale, Campania, Italy, plotted against the carbon-isotope record and the proposed intervals affected by the Plenus Cold Event and the mafic/volcanic/hydrothermal episode illustrated by relatively non-radiogenic osmium-isotope values. Legend as in Fig. 10. $^{87}Sr/^{86}Sr$ ratios decline through the OAE interval, suggesting relative increase in non-radiogenic strontium from mafic sources supplied to the oceans, as also indicated by the seawater osmium-isotope signature (Fig. 5). The increase in lithium-isotope ratios suggests accelerated weathering, most probably of a mafic source, given the trends in the strontium-isotope and osmium-isotope systems. The data are not such as to indicate any effect of the Plenus Cold Event. Strontium-isotope data, with internal errors plotted, are normalized to an NIST SRM-987 value of 0·710250. Data from Owens *et al.* (2013) and Pogge von Strandmann *et al.* (2013).

magmatic/mafic influences in controlling seawater ratios during the initial stages of OAE 2 and may also indicate an oceanic residence time less than the present-day figure of several million years. Nevertheless, the overall movement to less radiogenic values of both strontium and osmium isotopes over most of the OAE 2 interval indicates relative dominance of the mafic/magmatic signature that potentially masks the impact of increased continental weathering (Jones & Jenkyns, 2001; Turgeon & Creaser, 2008; Jenkyns, 2010; Du Vivier *et al.*, 2014, 2015).

The lithium-isotope signature is well-defined and shows a negative shift over the interval characterized by the osmium-isotope excursion to less radiogenic values. As noted above, movement to lower δ^7Li values is conventionally interpreted as due to intensified weathering of silicates, and the associated strontium-isotope and osmium-isotope signatures suggest that these minerals may have derived primarily from mafic rather than felsic (i.e. continental) rocks (Pogge von Strandmann *et al.*, 2013). As is the case with the Eastbourne Chalk section, such data suggest that construction/erosion of a LIP or LIPs was a significant process operating as a trigger for OAE 2, possibly accompanying accelerated global sea-floor spreading rates and hydrothermal activity (Jones & Jenkyns, 2001).

Molybdenum and uranium

The stratigraphic distribution of the redox-sensitive elements molybdenum and uranium is such as to show relatively low Mo/Ca and U/Ca ratios

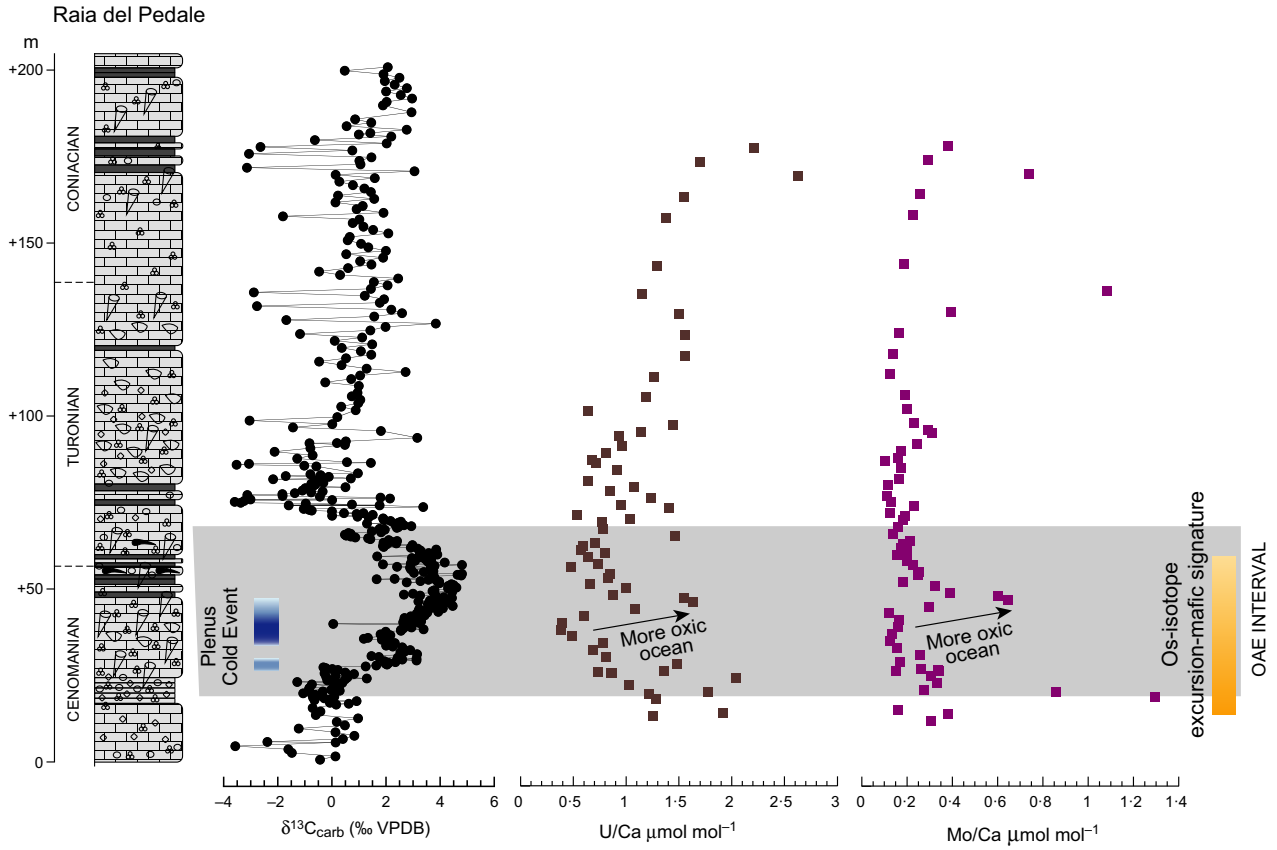

Fig. 12. Molybdenum/calcium and uranium/calcium ratios of platform carbonates from Raia del Pedale, Campania, Italy, plotted against the carbon-isotope record and the proposed intervals affected by the Plenus Cold Event and the mafic/volcanic/hydrothermal episode illustrated by relatively non-radiogenic osmium-isotope values. Legend as in Fig. 10. Both proxies show relatively low values over the interval of the OAE, probably reflecting global drawdown because of the widespread distribution of dysoxic, anoxic and euxinic environments in the world ocean. The rise in values seen in both Mo/Ca and U/Ca ratios corresponds with the proposed position of the Plenus Cold Event that must have allowed temporary expansion of global oxygenated waters, hence reducing the volume of sinks available for these two redox-sensitive metals, probably supplied by basalt–seawater interaction. There is no apparent relationship between the Plenus Cold Event and the osmium-isotope profiles.

over the OAE interval, except for a pronounced positive excursion in both profiles that begins at the mid-level of the major phase of the Plenus Cold Event (Fig. 12). In both parts of the section, the U/Ca data are generally the more scattered, whereas the Mo/Ca data more clearly outline the positive excursions. Both U and Mo, which today have near-uniform global concentrations and similar residence times of close to a million years (Broecker & Peng, 1982) in present-day seawater, are readily taken into organic-rich sediments, the former under suboxic conditions, the latter under euxinic conditions (Algeo & Tribovillard, 2009). Organic-rich sediments deposited during OAE 2 show elevated concentrations of both these elements relative to crustal abundances, with enrichment factors being typically greater for Mo than for U (Tribovillard *et al.*, 2012). However, during OAE 2 when organic-rich sediments were globally distributed and euxinic environments widely developed in the South Atlantic (Jenkyns, 2010), global drawdown of these two elements would have taken place, a phenomenon registered in organic-rich shales from ODP Site 1260 on Demerara Rise in the equatorial Atlantic that show relatively low values with respect to sediments stratigraphically above and below (van Bentum *et al.*, 2009; Hetzel *et al.*, 2009). Hence, the well-defined overall depletion in the U/Ca profile from Raia del Pedale over the OAE interval with recovery higher in the section (less obvious with the Mo/Ca data) is as predicted. However, the levels of increased concentrations of Mo and U that correlate stratigraphically with the Plenus Cold Event must indicate renewed oxygenation of depositional settings in the world ocean and concomitant reduction in the amount of, or efficiency of, suboxic to euxinic sinks and/or oxidation of previously deposited organic-rich sediments, allowing increases in dissolved concentrations of these redox-sensitive species, as was apparently also the case with a range of metal elements in the Eastbourne Chalk section (Fig. 8). Environmental change in the Raia del Pedale and other platform-carbonate successions at the level of the Plenus Cold Event is also indicated by a wave of benthonic foraminiferal extinctions (Parente *et al.*, 2008). A small positive excursion of Mo/Ca and U/Ca in the mid-Turonian may indicate a significant regional episode of re-oxygenation. There is no obvious relationship between the osmium-isotope profile and the Mo/Ca and U/Ca profiles.

COMPARATIVE OCEANIC ANOXIC EVENT 2 CHEMOSTRATIGRAPHY OF CYCLICALLY BEDDED ORGANIC-RICH SHALES AND LIMESTONES, TARFAYA, MOROCCO

Molybdenum and $\delta^{98/95}$Mo

The Tarfaya Basin, Morocco, represents an organic-rich shelf-sea site that has been much studied for Late Cretaceous palaeoceanography. Cyclic variations in nutrient availability from weathering of source-lands and/or upwelling intensity are thought to have been a major control on the nature of the sedimentary record, particularly in governing the ratio of laminated black shale to lighter coloured bioturbated carbonate (Kuhnt *et al.*, 1997, 2005; Tsikos *et al.*, 2004; Kolonic *et al.*, 2005; Poulton *et al.*, 2015). Molybdenum and molybdenum-isotope stratigraphy of the calcareous organic-rich sediments from a borehole at Tarfaya plotted against organic-carbon-isotope stratigraphy (Fig. 13) show no obvious relation to the seawater osmium-isotope signature but are manifestly influenced by the Plenus Cold Event (Dickson *et al.*, 2016). Most striking is a dramatic fall in molybdenum concentrations over this interval, readily interpreted as due to local oxygenation of the sea-floor hindering removal of the element into organic matter and sulphides because of the temporary absence of euxinic (i.e. sulphidic) conditions in the overlying watermass (Algeo & Lyons, 2006; Tribovillard *et al.*, 2012). Although unusual boreal ammonites are a feature of outcrops at Tarfaya, potentially implying the influence of the Plenus Cold Event, their position against a detailed stratigraphy is unclear, possibly because persistent upwelling of cool waters was an important palaeoceanographic factor at this locality (Einsele & Wiedman, 1982; Kuhnt *et al.*, 1986).

However, direct evidence for a phase of re-oxygenation is provided by the increased abundance of benthic foraminifera at the level of minimum Mo concentration and the specific recognition of the Benthic Oxic Event (Kuhnt *et al.*, 2005; Keller *et al.*, 2008). Under such conditions, Fe-oxyhydroxides and Mn-oxyhydroxides may have been rendered temporarily stable, allowing preferred incorporation of ^{95}Mo into the sediment and hence explaining the negative molybdenum-isotope excursion that correlates with lower contents of the element itself (Dickson *et al.*, 2016). In fact, the ultra-high-resolution study by Goldberg *et al.* (2016) clearly shows two distinct shifts

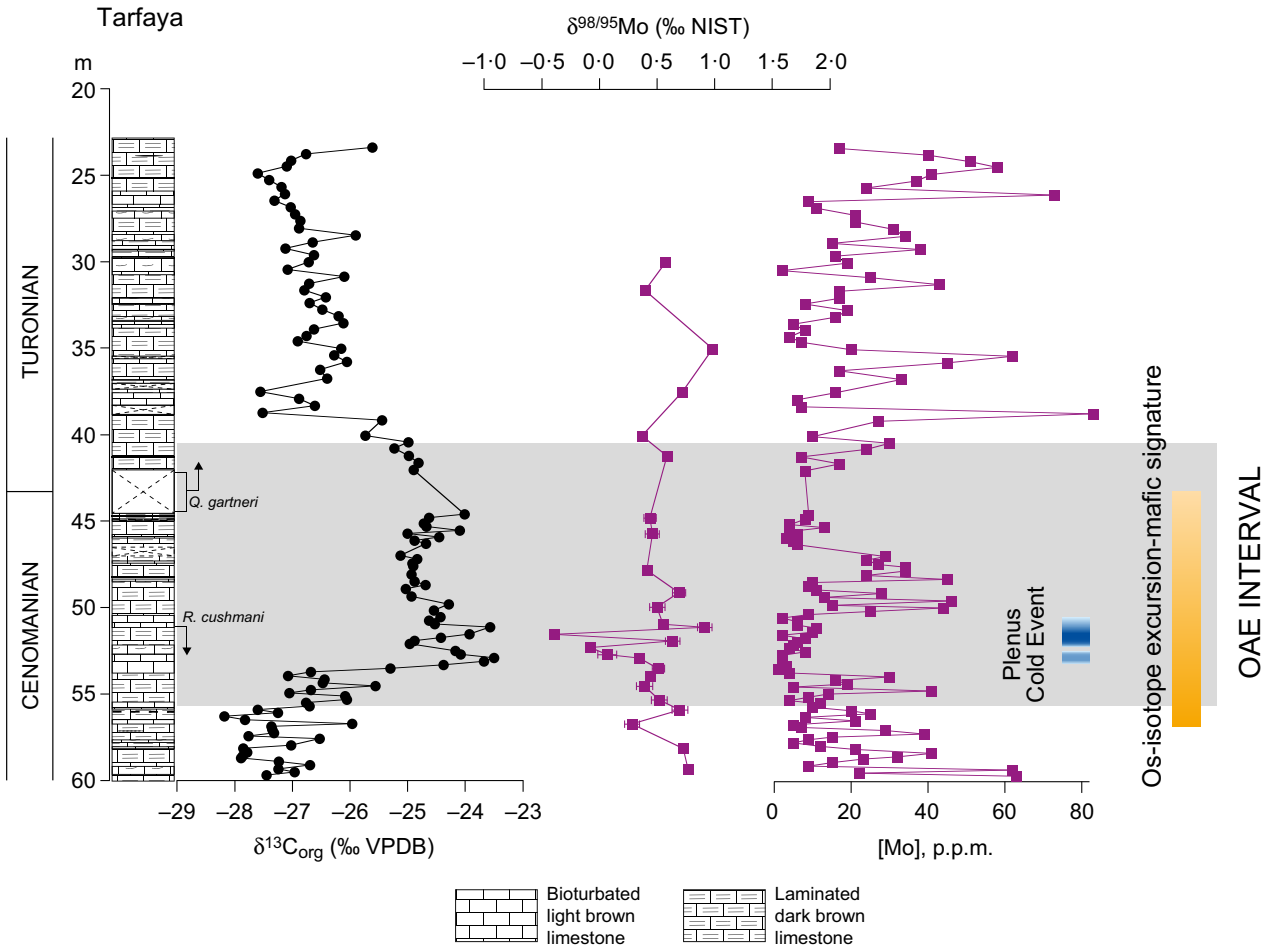

Fig. 13. Molybdenum abundance and molybdenum-isotope ($\delta^{98/95}$Mo) ratios of cyclically bedded organic-rich shales and limestones from Tarfaya plotted against the carbon-isotope record and the proposed intervals affected by the Plenus Cold Event and the mafic/volcanic/hydrothermal episode illustrated by relatively non-radiogenic osmium-isotope values. Brick ornament represents bioturbated light brown limestone; brick ornament with dashes represents darker more laminated limestone. The stratigraphic level showing lowest molybdenum abundances correlates well with the interval recording the Plenus Cold Event and is consistent with movement of the molybdenum-isotope ratio to lower values due to preferential fractionation of the light isotope from seawater into local relatively oxic sinks recorded by the section. There is no apparent relationship with the osmium-isotope profile. The end-level of the OAE interval is placed where the definite drop in carbon-isotope values begins, which is stratigraphically higher than the position suggested by Tsikos *et al.* (2004). Additional data from Dickson *et al.* (2016).

to lower values that correlate with the inferred stratigraphic interval that records the two proposed pulses of the Plenus Cold Event.

These molybdenum-isotope trends are not observed in deep Atlantic and Tethyan sites (Westermann *et al.*, 2014; Dickson *et al.*, 2016), even though the Plenus Cold Event is locally registered in Demerara Rise by repopulation of the sediment by benthonic foraminifera (Friedrich *et al.*, 2006), suggesting that the impact of seafloor re-oxygenation was more significant at shallower shelf-sea sites than in the deeper parts of oceans and their margins. Unlike the Mo profile from Raia del Pedale, which is taken to record dissolved concentrations of this metal in global seawater, the values from Tarfaya have been controlled primarily by local redox conditions governing the degree of authigenic enrichment and isotopic fractionation.

CONCLUSIONS

The geochemistry of Oceanic Anoxic Event 2 (OAE 2) is complex, although the principal geochemical themes involve some kind of interaction between mafic igneous rock, presumably primarily basalt, and seawater that began prior to

the positive shift in marine carbon-isotope ratios, taken to define the onset of the event. Given that the diagnostic osmium-isotope ratios remain relatively low throughout most of the event before abruptly rebounding to higher values, this interaction persisted over hundreds of thousands of years. Drawdown of carbon dioxide due to weathering of silicates, both mafic and silicic, as well as carbon burial itself must not have outpaced any volcanogenic supply of this greenhouse gas, in order to maintain relatively high temperatures, except during the interval/s of the Plenus Cold Event, during which a range of redox-related geochemical phenomena took place. The overlap in time between the trace-element 'spikes' seen in sections from Europe and North America and the Plenus Cold Event suggests that, during this interval, ongoing basalt–seawater interaction combined with loss of global anoxic/euxinic sinks and/or oxidation of previously deposited organic matter and pyrite introduced a host of redox-sensitive metals to seawater that were captured in carbonate sediments deposited under oxic conditions. The following conclusions may be drawn:

1 The Plenus Cold Event during the Cenomanian–Turonian (C/T) OAE can be separated, at least locally, into two cooler pulses, separated by a warmer interval.

2 The relatively mafic signatures (strontium isotopes, osmium isotopes, neodymium isotopes and some trace elements) of the C/T OAE probably record construction and/or destruction of one or more Large Igneous Provinces (LIPs). The osmium-isotope anomaly clearly pre-dates the onset level of the Oceanic Anoxic Event, allowing whatever produced the former as a causative agent for the latter.

3 The calcium-isotope and lithium-isotope signatures of the C/T OAE (Eastbourne and Raia del Pedale) spotlight the importance of accelerated silicate weathering during Oceanic Anoxic Event 2, probably involving subaerial destruction of a Large Igneous Province as well as continental rocks.

4 The Mn/Ca ratios characteristic of the C/T OAE record the local suboxic conditions below the floor of the Chalk Sea during the OAE (Eastbourne), with manganese possibly derived from mafic sources and not drawn down into regionally deposited organic-rich shales.

5 The sulphur-isotope (CAS) signature of the C/T OAE (Eastbourne and Raia del Pedale) could also record volcanic/hydrothermal (mafic) influence coincident with the osmium-isotope anomaly and/or oxidation of sedimentary pyrite during the Plenus Cold Event.

6 The Ce/Ca ratios characteristic of the C/T OAE record the regional to global spread of anoxic to euxinic waters but also re-oxygenation of local seawater (Eastbourne) during the Plenus Cold Event. The Ce/Ca record at the shallow-water Raia del Pedale site is more problematic and may reflect the local presence of oxic sinks in a carbonate-platform environment.

7 The I/Ca ratios characteristic of the C/T OAE record the local re-oxygenation of the Chalk Sea (Eastbourne) during the Plenus Cold Event.

8 The Mo and U contents of limestones from Raia del Pedale, albeit showing relative depletion over the OAE interval probably due to global drawdown of these trace elements, record the Plenus Cold Event by showing relative enrichment in seawater at this level.

9 Oxidation of previously deposited organic matter and pyrite during the Plenus Cold Event, as well as continued basalt–seawater interaction recorded in the global osmium-isotope ratios, is credited with enriching global ocean waters with a range of redox-sensitive trace metals (V, Cr, Co, Ni, Cu, Zn and Cd). Under these circumstances, organic-rich shales deposited during the early phase of the OAE may have acted as a geochemical capacitor for these elements.

10 The Mo contents and molybdenum-isotope ratios of the C/T OAE at Tarfaya record decreased input of this element into sediment under the relatively more oxic conditions of the Plenus Cold Event and preferred local enrichment of that sediment with the lighter isotope (^{95}Mo).

ACKNOWLEDGEMENTS

We thank Steve Wyatt, Peter Ditchfield, Phil Holdship and Alan Hsieh for laboratory support and Shell for funding. Earlier collaborative work with Zunli Lu, Jeremy Owens, Philip Pogge von Strandmann and Harry Tsikos is also acknowledged. Comments by three reviewers are gratefully acknowledged.

REFERENCES

Adams, D., **Hurtgen, M.T.** and **Sageman, B.B.** (2010) Volcanic triggering of a biogeochemical cascade during Oceanic Anoxic Event 2. *Nat. Geosci.*, **3**, 201–204.

Algeo, T.J. and **Lyons, T.W**. (2006) Mo–total organic carbon covariation in modern anoxic marine environments: implications for analysis of paleoredox and paleohydrographic conditions. *Paleoceanography*, **21**, PA2016. doi: 10.1029/2004PA001112.

Algeo, T.J. and **Tribovillard, N.** (2009) Environmental analysis of paleoceanographic systems based on molybdenum–uranium covariation. *Chem. Geol.*, **268**, 211–225.

Ando, A., **Nakano, T.**, **Kaiho, K.**, **Kobayashi, T.**, **Kokado, E.** and **Khim, B.-K.** (2009) Onset of seawater 87Sr/86Sr excursion prior to Cenomanian-Turonian Oceanic Anoxic Event 2? New Late Cretaceous strontium isotope curve from the central Pacific Ocean. *J. Foram. Res.*, **39**, 322–334.

Arkhanguelsky, A.D. (1916) Le Crétacé supérieur du Turkestan. Livraison première. Le Crétacé supérieur du nord-ouest du désert Kyzl-Koum et du Fergana (in Russian). *Mémoires du Comité géologique, Nouvelle Série, Petrograd*, **151**, 98.

Arthur, M.A., **Jenkyns, H.C.**, **Brumsack, H.-J.** and **Schlanger, S.O**. (1990) Stratigraphy, geochemistry, and paleoceanography of organic carbon-rich Cretaceous sequences. In: *Cretaceous Resources, Events and Rhythms* (Eds R.N. Ginsburg and B. Beaudoin), NATO ASI Ser. C, vol. 304, pp. 75–119. Kluwer Academic Publishers, Dordrecht.

Barclay, R.S., **McElwain, J.C.** and **Sageman, B.B.** (2010) Carbon sequestration activated by a volcanic CO_2 pulse during ocean anoxic event 2. *Nat. Geosci.*, **3**, 205–208.

van Bentum, E.C., **Hetzel, A.**, **Brumsack, H.-J.**, **Forster, A.**, **Reichart, G.-J.** and **Sinninghe Damsté, J.S.** (2009) Reconstruction of water column anoxia in the equatorial Atlantic during the Cenomanian-Turonian Oceanic Anoxic Event using biomarker and trace metal proxies. *Palaeogeogr. Palaeoclimatol. Palaeoecol.*, **280**, 489–498.

Berner, R.A. (1981) Authigenic mineral formation resulting from organic matter decomposition in modern sediments. *Fortschr. Mineral.*, **59**, 117–135.

Blättler, C.L., **Jenkyns, H.C.**, **Reynard, L.M.** and **Henderson, G.M.** (2011) Significant increases in global weathering during Oceanic Anoxic Events 1a and 2 indicated by calcium isotopes. *Earth Planet. Sci. Lett.*, **309**, 77–88.

Bodin, S., **Godet, A.**, **Westermann, S.** and **Föllmi, K.B.** (2013) Secular change in northwestern Tethyan water-mass oxygenation during the late Hauterivian–early Aptian. *Earth Planet. Sci. Lett.*, **374**, 121–131.

Bottrell, S.H. and **Newton, R.J.** (2006) Reconstruction of changes in global sulfur cycling from marine sulfate isotopes. *Earth Sci. Rev.*, **75**, 59–83.

Bralower, T.J., **Arthur, M.A.**, **Leckie, R.M.**, **Sliter, W.V.**, **Allard, D.** and **Schlanger, S.O.** (1994) Timing and paleoceanography of oceanic dysoxia/anoxia in the late Barremian to early Aptian. *Palaios*, **9**, 335–369.

Bralower, T.J., **Fullagar, P.D.**, **Paull, C.K.**, **Dwyer, G.S.** and **Leckie, R.M.** (1997) Mid-Cretaceous strontium-isotope stratigraphy of deep-sea sections. *Geol. Soc. Am. Bull.*, **109**, 1421–1442.

Broecker, W.S. and **Peng, T.-H**. (1982) *Tracers in the Sea*. Eldigio Press, Lamont-Doherty Geological Observatory, New York, NY, 690 pp.

Brumsack, H.-J. (2006) The trace metal content of recent organic carbon-rich sediments: implications for Cretaceous black shale formation. *Palaeogeogr. Palaeoclimatol. Palaeoecol.*, **232**, 344–361.

Calvert, S.E. and **Pedersen, T.F.** (1996) Sedimentary geochemistry of manganese: implications for the environment of formation of manganiferous black shales. *Econ. Geol.*, **91**, 36–47.

Clarke, L. and **Jenkyns, H.C.** (1999) New oxygen isotope evidence for long-term Cretaceous climatic change in the Southern Hemisphere. *Geology*, **27**, 699–702.

Courtillot, V.E. and **Renne, P.R.** (2003) On the ages of flood basalt events. *C.R. Geosci.*, **335**, 113–140.

Crumière, J.-P., **Crumière-Airaud, C.** and **Espitalié, J**. (1990) Préservation cyclique de la matière organique amorphe des sédiments au passage Cénomanien–Turonien dans le Bassin vocontien (Sud-Est France). Contrôles paléo-océanographiques. *Bull. Soc. Géol. France*, série 8, **6**, 469–478.

Davey, S. and **Jenkyns, H.C.** (1999) Carbon-isotope stratigraphy of shallow-water limestones and implications for the timing of Late Cretaceous sea-level rise and anoxic events (Cenomanian-Turonian of the peri-Adriatic carbonate platform, Croatia). *Eclog. Geol. Helv.*, **92**, 163–170.

Dickens, G.R. and **Owen, R.M.** (1995) Rare element deposition in pelagic sediment at the Cenomanian-Turonian boundary, Exmouth Plateau. *Geophys. Res. Lett.*, **22**, 203–206.

Dickson, A.J., **Jenkyns, H.C.**, **Porcelli, D.**, **van den Boorn, S.** and **Idiz, E.** (2016) Basin-scale controls on the molybdenum-isotope composition of seawater during Oceanic Anoxic Event 2 (Late Cretaceous). *Geochim. Cosmochim. Acta*, **178**, 291–306.

Dickson, A.J., **Saker-Clark, M.**, **Jenkyns, H.C.**, **Bottini, C.**, **Erba, E.**, **Russo, F.**, **Gorbanenko, O.**, **Naafs, B.D.A.**, **Pancost, R.D.**, **Robinson, S.A.** and **van den Boorn, S.H.J.M**. (2017) A Southern Hemisphere record of global trace-metal drawdown and orbital modulation of organic-matter burial across the Cenomanian–Turonian boundary (ODP Site 1138, Kerguelen Plateau). *Sedimentology*, **64**, in press. doi: 10.1111/sed.12303.

Du Vivier, A., **Selby, D.**, **Sageman, B.B.**, **Jarvis, I.**, **Gröcke, D.R.** and **Voigt, S.** (2014) Marine $^{187}Os/^{188}Os$ isotope stratigraphy reveals the interaction of volcanism and ocean circulation during Oceanic Anoxic Event 2. *Earth Planet. Sci. Lett.*, **389**, 23–33.

Du Vivier, A., **D. Selby, D.**, **Condon, D.J.**, **Takashima, R.** and **Nishi, H**. (2015) Pacific $^{187}Os/^{188}Os$ isotopic chemistry and U–Pb geochronology: synchroneity of global Os isotope change across OAE 2. *Earth Planet. Sci. Lett.*, **428**, 204–216.

Eicher, D.L. and **Worstell, P.** (1970) Cenomanian and Turonian foraminifera from the Great Plains, United States. *Micropaleontology*, **16**, 269–324.

Einsele, G. and **Wiedman, J.** (1982) Turonian black shales in the Moroccan coastal basins: first upwelling in the Atlantic Ocean? In: *Geology of the Northwest African Margin* (Eds U. von Rad, K. Hinz, M. Sarnhein and E. Sebold), pp. 396–414. Springer-Verlag, Berlin.

Elderbak, K., **Leckie, R.M.** and **Tibert, N.E.** (2014) Paleoenvironmental and paleoceanographic changes across the Cenomanian-Turonian Boundary Event (Oceanic Anoxic Event 2) as indicated by foraminiferal assemblages from the eastern margin of the Cretaceous Western Interior Sea. *Palaeogeogr. Palaeoclimatol. Palaeoecol.*, **413**, 29–48.

Elderfield, H. and **Greaves, M.J.** (1982) The rare earth elements in seawater. *Nature*, **296**, 214–219.

Eldrett, J.S., **Minisini, D.** and **Bergman, S.C.** (2014) Decoupling of the carbon cycle during ocean anoxic event 2. *Geology*, **42**, 567–570.

Eldrett, J.S., **Ma, C.**, **Bergman, S.C.**, **Lutz, B.**, **Gregory, F.J.**, **Dodsworth, P.**, **Phipps, M.**, **Hardas, P.**, **Minisini, D.**, **Ozkan, A.**, **Ramezani, J.**, **Bowring, S.A.**, **Kamo, S.L.**, **Ferguson, K.**, **Macaulay, C.** and **Kelly, A.E.** (2015) An astronomically calibrated stratigraphy of the Cenomanian, Turonian and earliest Coniacian from the Cretaceous Western Interior Seaway, USA: implications for global chronostratigraphy. *Cretaceous Res.*, **56**, 316–344.

Elrick, M., **Molina-Garza, R.**, **Duncan, R.** and **Snow, L.** (2009) C-isotope stratigraphy and paleoenvironment changes across OAE2 (mid-Cretaceous) from shallow-water platform carbonates of southern Mexico. *Earth Planet. Sci. Lett.*, **277**, 295–306.

Erba, E., **Duncan, R.A.**, **Bottini, C.**, **Tiraboschi, D.**, **Weissert, H.**, **Jenkyns, H.C.** and **Malinverno, A**. (2015) Environmental consequences of Ontong Java Plateau and Kerquelen Plateau volcanism. In: *The Origin, Evolution, and environmental Consequences of Oceanic Large Igneous Provinces* (Eds C.R. Neal, W.W. Sager, T. Sano and E. Erba), *Geol. Soc. Am. Spec. Paper*, **511**, 271–303.

Erbacher, J., **Friedrich, O.**, **Wilson, P.A.**, **Birch, H.** and **Mutterlose, J.** (2005) Stable organic carbon isotope stratigraphy across Oceanic Anoxic Event 2 of Demerara Rise, western tropical Atlantic. *Geochem. Geophys. Geosyst.*, **6**, Q06010. doi:10.1029/2004GC000850.

Forster, A., **Schouten, S.**, **Baas, M.** and **Sinninghe Damsté, J.S.** (2007a) Mid-Cretaceous (Albian–Santonian) sea surface temperature record of the tropical Atlantic Ocean. *Geology*, **35**, 919–922.

Forster, A., **Schouten, S.**, **Moriya, K.**, **Wilson, P.A.** and **Sinninghe Damsté, J.S**. (2007b) Tropical warming and intermittent cooling during the Cenomanian/Turonian Oceanic Anoxic Event 2: sea surface temperature records from the equatorial Atlantic. *Paleoceanography*, **22**, PA 1219. doi: 10.1029/2006PA001349.

Friedrich, O., **Erbacher, J.** and **Mutterlose, J.** (2006) Paleoenvironmental changes across the Cenomanian/Turonian Boundary Event (Oceanic Anoxic Event 2) as indicated by benthic foraminifera from the Demerara Rise (ODP Leg 207). *Rev. Micropaléontol.*, **49**, 121–139.

Friedrich, O., **Norris, R.D.** and **Erbacher, J.** (2012) Evolution of middle to Late Cretaceous oceans—a 55 m.y. record of Earth's temperature and carbon cycle. *Geology*, **40**, 107–110.

Frijia, G. and **Parente, M.** (2008) Strontium isotope stratigraphy in the upper Cenomanian shallow-water carbonates of the southern Apennines: short-term perturbations of marine $^{87}Sr/^{86}Sr$ during the Oceanic Anoxic Event 2. *Palaeogeogr. Palaeoclimatol. Palaeoecol.*, **261**, 15–29.

Froelich, P.N., **Klinkhammer, G.P.**, **Bender, M.L.**, **Luedtke, N.A.**, **Heath, G.R.**, **Cullen, G.** and **Dauphin, P.** (1979) Early oxidation of organic matter in pelagic sediments of the eastern equatorial Atlantic: suboxic diagenesis. *Geochim. Cosmochim. Acta*, **43**, 1075–1090.

Gale, A.S. and **Christensen, W.K.** (1996) Occurrence of the belemnite *Actinocamax plenus* in the Cenomanian of SE France and its significance. *Bull. Geol. Soc. Denmark*, **43**, 68–77.

Gale, A.S., **Jenkyns, H.C.**, **Kennedy, W.J.** and **Corfield, R.M.** (1993) Chemostratigraphy versus biostratigraphy: data from around the Cenomanian-Turonian boundary. *J. Geol. Soc. London*, **150**, 29–32.

Gambacorta, G., **Jenkyns, H.C.**, **Russo, F.**, **Tsikos, H.**, **Wilson, P.A.** and **Erba, E.** (2015) Carbon- and oxygen-isotope records of mid-Cretaceous Tethyan pelagic sequences from the Umbria–Marche and Belluno Basins (Italy). *Newsl. Stratigr.*, **48**, 299–323.

Gavrilov, Yu.O, **Shcherbinina, E.A.**, **Golovanova, O.V.** and **Pokrovskii, B.G.** (2013) The Late Cenomanian Paleoecological Event (OAE 2) in the Eastern Caucasus Basin of northern Peri-Tethys. *Lithol. Min. Resour.*, **48**, 457–488.

German, C.R. and **Elderfield, H.** (1990) Application of the Ce anomaly as a paleoredox indicator: the ground rules. *Paleoceanography*, **5**, 823–833.

Goldberg, E.D., **Koide, M.**, **Schmitt, R.A.** and **Smith, R.H.** (1963) Rare-earth distributions in the marine environment. *J. Geophys. Res.*, **68**, 4209–4217.

Goldberg, T., **Poulton, S.W.**, **Wagner, T.**, **Kolonic, S.F.** and **Rehkämper, M.** (2016) Molybdenum drawdown during Cretaceous Oceanic Anoxic Event 2. *Earth Planet. Sci. Lett.*, **440**, 81–91.

Gomes, M.L., **Hurtgen, M.T.** and **Sageman, B.B.** (2016) Biogeochemical sulfur cycling during cretaceous ocean anoxic events: a comparison of OAE1a and OAE2. *Paleoceanography*, **31**, 233–251.

Hancock, J.M. (1975) The petrology of the Chalk. *Proc. Geol. Assoc.*, **86**, 499–535.

Hasegawa, T. (1997) Cenomanian-Turonian carbon isotope events recorded in terrestrial organic matter from northern Japan. *Palaeogeogr. Palaeoclimatol. Palaeoecol.*, **130**, 251–273.

van Helmond, N.A.G.M., **Sluijs, A.**, **Reichart, G.-J.**, **Sinninghe Damsté, J.S.**, **Slomp, C.P.** and **Brinkhuis, H.** (2013) A perturbed hydrological cycle during Oceanic Anoxic Event 2. *Geology*, **42**, 123–126.

van Helmond, N.A.G.M., **Ruvalcaba, I.**, **Sluijs, A.**, **Sinninghe Damsté, J.S.** and **Slomp, C.P.** (2014) Spatial extent and degree of oxygen depletion in the deep proto-North Atlantic basin during Oceanic Anoxic Event 2. *Geochem. Geophys. Geosyst.*, **15**, 4254–4266.

van Helmond, N.A.G.M., **Sluijs, A.**, **Sinninghe Damsté, J.S.**, **Reichart, G.-J.**, **Voigt, S.**, **Erbacher, J.**, **Pross, J.** and **Brinkhuis, H.** (2015) Freshwater discharge controlled deposition of Cenomanian-Turonian black shales on the NW European epicontinental shelf (Wunstorf, northern Germany). *Clim. Past*, **11**, 495–508.

van Helmond, N.A.G.M., **Sluijs, A.**, **Papadomanolaki, N.M.**, **Plint, A.G.**, **Gröcke, D.**, **Pearce, M.A.**, **Eldrett, J.S.**, **Trabucho-Alexandre, J.**, **de Walaszczyk van Schootbrugge, B.** and **Brinkhuis, H**. (2016) Equatorward phytoplankton migration during a cold spell within the Late Cretaceous super-greenhouse. *Biogeosciences*, **13**, 2859–2872.

Hetzel, A., **Böttcher, M.E.**, **Wortmann, U.G.** and **Brumsack, H.-J.** (2009) Paleo-redox conditions during OAE 2 reflected in Demerara Rise sediment geochemistry (ODP Leg 207). *Palaeogeogr. Palaeoclimatol. Palaeoecol.*, **273**, 302–308.

Holmden, C., **Jacobson, A.D.**, **Sageman, B.B.** and **Hurtgen, M.T.** (2016) Response of the Cr isotope proxy to Cretaceous Oceanic Anoxic Event 2 in a pelagic carbonate succession from the Western Interior Seaway. *Geochim. Cosmochim. Acta*, **186**, 277–295.

Holser, W.T. (1997) Evaluation of the application of rare-earth elements to paleoceanography. *Palaeogeogr. Palaeoclimatol. Palaeoecol.*, **132**, 309–323.

Holser, W.T. and **Kaplan, I.R**. (1966) Isotope geochemistry of sedimentary sulfates. *Chem. Geol.*, **1**, 93–135.

Huber, B.T., **Norris, R.D.** and **MacLeod, K.G.** (2002) Deep-sea paleotemperature record of extreme warmth during the Cretaceous. *Geology*, **30**, 123–126.

Jarvis, I., **Murphy, A.M.** and **Gale, A.S.** (2001) Geochemistry of pelagic and hemipelagic carbonates: criteria for identifying systems tracts and sea-level change. *J. Geol. Soc. London*, **158**, 685–696.

Jarvis, I., **Gale, A.S.**, **Jenkyns, H.C.** and **Pearce, M.A.** (2006) Secular variation in Late Cretaceous carbon isotopes: a new δ13C carbonate reference curve for the Cenomanian-Campanian (99.6–70.6 Ma). *Geol. Mag.*, **143**, 561–608.

Jarvis, I., **Lignum, J.S.**, **Gröcke, D.R.**, **Jenkyns, H.C.** and **Pearce, M.A**. (2011) Black shale deposition, atmospheric CO_2 drawdown and cooling during the Cenomanian-Turonian Oceanic Anoxic Event. *Paleoceanography*, **26**, PA3201. doi: 10.1029/2010PA002081.

Jeans, C.V., **Long, D.**, **Hall, M.A.**, **Bland, D.J.** and **Cornford, C.** (1991) The geochemistry of the Plenus Marls at Dover, England: evidence of fluctuating oceanographic conditions and of glacial control during the development of the Cenomanian-Turonian $\delta^{13}C$ anomaly. *Geol. Mag.*, **128**, 603–632.

Jefferies, R.P.S. (1961) The palaeoecology of the Actinocamax Plenus Subzone (Turonian) in the Anglo-Paris Basin. *Palaeontology*, **4**, 609–647.

Jefferies, R.P.S. (1963) The stratigraphy of the *Actinocamax Plenus* Subzone (Lowest Turonian) in the Anglo-Paris Basin. *Proc. Geol. Ass.*, **74**, 1–33.

Jeletsky, J.A. (1950) Actinocamax from the Upper Cretaceous of Manitoba. *Bull. Geol. Surv. Canada*, **15**, 1–27.

Jenkyns, H.C. (1980) Cretaceous anoxic events: from continents to oceans. *J. Geol. Soc. London*, **137**, 171–188.

Jenkyns, H.C. (2003) Evidence for rapid climate change in the Mesozoic-Palaeogene greenhouse world. *Phil. Trans. R Soc. London A*, **361**, 1885–1916.

Jenkyns, H.C. (2010) Geochemistry of Oceanic Anoxic Events. *Geochem. Geophys. Geosyst.*, **11**, Q03004. doi:10.1029/2009GC002788.

Jenkyns, H.C., **Gale, A.S.** and **Corfield, R.M.** (1994) Carbon- and oxygen-isotope stratigraphy of the English Chalk and Italian Scaglia and its palaeoclimatic significance. *Geol. Mag.*, **131**, 1–34.

Jones, C.E. and **Jenkyns, H.C.** (2001) Seawater strontium isotopes, Oceanic Anoxic Events, and seafloor hydrothermal activity in the Jurassic and Cretaceous. *Am. J. Sci.*, **301**, 112–149.

Joo, Y.J. and **Sageman, B.B.** (2014) Cenomanian to Campanian carbon isotope chemostratigraphy from the Western Interior Basin. *J. Sed. Res.*, **84**, 529–542.

Keller, G. and **Pardo, A.** (2004) Age and paleoenvironment of the Cenomanian-Turonian global stratotype section and point at Pueblo, Colorado. *Mar. Micropaleont.*, **51**, 95–128.

Keller, G., **Adatte, T.**, **Berner, Z.**, **Chellai, E.H.** and **Stueben, D.** (2008) Oceanic events and biotic effects of the Cenomanian-Turonian anoxic event, Tarfaya Basin, Morocco. *Cretaceous Res.*, **29**, 976–994.

Kennedy, W.J., **Walaszczyk, I.** and **Cobban, W.A.** (2005) The global boundary stratotype section and point for the base of the Turonian Stage of the Cretaceous: Pueblo, Colorado. *Episodes*, **28**, 93–104.

Kerr, A.C. (1998) Oceanic plateau formation: a cause of mass extinction and black shale deposition around the Cenomanian–Turonian boundary. *J. Geol. Soc. London*, **155**, 619–626.

Kolonic, S., **Wagner, T.**, **Forster, A.**, **Sinninghe Damsté, J. S.**, **Walsworth-Bell, B.**, **Erba, E.**, **Turgeon, S.**, **Brumsack, H.**, **Chellai, E.H.**, **Tsikos, H.**, **Kuhnt, W.** and **Kuypers, M. M. M**. (2005) Black shale deposition on the northwest African Shelf during the Cenomanian/Turonian Oceanic Anoxic Event: climate coupling and global organic carbon burial. *Paleoceanography*, **20**, PA1006. doi:10.1029/2003PA000950.

Košťák, M. and **Wiese, F.** (2008) Lower Turonian record of belemnite *Praeactinocamax* from NW Siberia and its palaeogeographic significance. *Acta Palaeontol. Pol.*, **53**, 669–678.

Košťák, M., **Čech, S.**, **Ekrt, B.**, **Mazuch, M.**, **Wiese, F.**, **Voigt, S.** and **Wood, C.J.** (2004) Belemnites of the Bohemian Cretaceous Basin in a global context. *Acta Geol. Pol.*, **54**, 511–533.

Kuhnt, W., **Thurow, J.**, **Wiedman, J.** and **Herbin, J.P**. (1986) Oceanic anoxic conditions around the Cenomanian/Turonian boundary and the response of the biota. In: *Biogeochemistry of Black Shales* (Eds E.T. Degens, P.A. Meyers and S.C. Brassell), *Mitt. Geol.-Paläont. Univ. Hamburg*, **60**, 205–246.

Kuhnt, W., **Nederbragt, A.** and **Leine, L.** (1997) Cyclicity of Cenomanian-Turonian organic-carbon-rich sediments in the Tarfaya Atlantic Coastal Basin (Morocco). *Cretaceous Res.*, **18**, 587–601.

Kuhnt, W., **Luderer, F.**, **Nederbragt, S.**, **Thurow, J.** and **Wagner, T.** (2005) Orbital-scale record of the late Cenomanian-Turonian Oceanic Anoxic Event (OAE-2) in the Tarfaya Basin (Morocco). *Int. J. Earth Sci.*, **94**, 147–159.

Kuroda, J., **Ogawa, N.O.**, **Tanimizu, M.**, **Coffin, M.F.**, **Tokuyama, H.**, **Kitazato, H.** and **Ohkouchi, N.** (2007) Contemporaneous massive subaerial volcanism and late Cretaceous Oceanic Anoxic Event 2. *Earth Planet. Sci. Lett.*, **256**, 211–223.

Kuypers, M.M.M., **Pancost, R.D.** and **Sinninghe Damsté, J.S.** (1999) A large and abrupt fall in atmospheric CO_2 concentration during Cretaceous times. *Nature*, **399**, 342–345.

Lamolda, M.A., **Gorostidi, A.** and **Paul, C.R.C.** (1994) Quantitative estimates of calcareous nannofossil changes across the Plenus Marls (latest Cenomanian), Dover, England: implications for the generation of the Cenomanian-Turonian Boundary Event. *Cretaceous Res.*, **15**, 143–164.

Lenniger, M., **Nøhr-Hansen Hills, L.V.** and **Bjerrum, C.J**. (2014) Arctic black shale formation during Cretaceous Oceanic Anoxic Event 2. *Geology*, **42**, 799–802.

Li, X., **Jenkyns, H.C.**, **Wang, C.**, **Hu, X.**, **Chen, X.**, **Wei, Y.**, **Huang, Y.** and **Cui, J.** (2006) Upper Cretaceous carbon-and oxygen-isotope stratigraphy of hemipelagic carbonate facies from southern Tibet, China. *J. Geol. Soc. London*, **163**, 375–382.

Lu, Z., **Jenkyns, H.C.** and **Rickaby, R.E.M.** (2010) Iodine to calcium ratios in marine carbonate as a paleo-redox proxy during Oceanic Anoxic Events. *Geology*, **38**, 1107–1110.

Ma, C., **Meyers, S.R.**, **Sageman, B.B.**, **Singer, B.S.** and **Jicha, B.R.** (2014) Testing the astronomical time scale for Oceanic Anoxic Event 2, and its extension into Cenomanian strata of the Western Interior Basin (USA). *Geol. Soc. Am. Bull.*, **126**, 974–989.

Martin, E.E., **MacLeod, K.G.**, **Jiménez Berrocoso, A.** and **Bourbon, E**. (2012) Water mass circulation on Demerara rise during the Late Cretaceous based on Nd isotopes. *Earth Planet. Sci. Lett.*, **327–328**, 111–120.

McArthur, J.M., **Thirlwall, M.F.**, **Gale, A.S.**, **Kennedy, W.J.**, **Burnett, J.A.**, **Mattey, D.** and **Lord, A. R**. (1993) Strontium

isotope stratigraphy for the Late Cretaceous: a new curve based on the English Chalk. In: *High Resolution Stratigraphy* (Eds E. Hailwood and R. Kidd), *Geol. Soc. London. Spec. Publ.*, **70**, 195–209.

McArthur, J.M., **Kennedy, W.J.**, **Chen, M.**, **Thirlwall, M.F.** and **Gale, A.S.** (1994) Strontium isotope stratigraphy for the Late Cretaceous: direct numerical age calibration of the Sr-isotope curve for the U.S. Western Interior Seaway. *Palaeogeogr. Palaeoclimtol. Palaeoecol.*, **108**, 95–119.

Meyers, S.R., **Siewert, S.E.**, **Singer, B.S.**, **Sageman, B.B.**, **Condon, D.J.**, **Obradovich, J.D.**, **Jicha, B.R.** and **Sawyer, D.A.** (2012) Intercalibration of radioisotopic and astrochronologic time scales for the Cenomanian-Turonian boundary interval, Western Interior Basin, USA. *Geology*, **40**, 7–10.

Misra, S. and **Froelich, P.N.** (2012) Lithium isotope history of Cenozoic seawater: changes in silicate weathering and reverse weathering. *Science*, **335**, 818–823.

Norris, R.D., **Bice, K.L.**, **Magno, E.A.** and **Wilson, P.A.** (2002) Jiggling the tropical thermostat in the Cretaceous hothouse. *Geology*, **30**, 299–302.

Ogg, J.G. and **Hinnov, L.A.** (2012) Cretaceous. In: *The Geologic Time Scale 2012* (Eds F.M. Gradstein, J.G. Ogg, M. Schmitz and G.M. Ogg), pp. 793–853. Elsevier, Amsterdam.

Ohkouchi, N., **Kawamura, K.**, **Kajiwara, Y.**, **Wada, E.**, **Okada, M.**, **Kanamatsu, T.** and **Taira, A.** (1999) Sulfur isotope records around Livello Bonarelli (northern Apennines, Italy) black shale at the Cenomanian-Turonian boundary. *Geology*, **27**, 535–538.

Orth, C.J., **Attrep, M.**, **Quintana, L.R.**, **Elder, W.P.**, **Kauffman, E.G.**, **Diner, R.** and **Villamil, T.** (1993) Elemental abundance anomalies in the late Cenomanian extinction interval: a search for the source(s). *Earth Planet. Sci. Lett.*, **117**, 189–204.

Owens, J.D., **Gill, B.C.**, **Jenkyns, H.C.**, **Bates, S.M.**, **Severmann, S.**, **Kuypers, M.M.M.**, **Woodfine, R.G.** and **Lyons, T.W.** (2013) Sulfur isotopes track the global extent and dynamics of euxinia during Cretaceous Oceanic Anoxic Event 2. *Proc. Natl Acad. Sci. USA*, **110**, 18407–18412.

Parente, M., **Frijia, G.**, **Di Lucia, M.**, **Jenkyns, H.C.**, **Woodfine, R.G.** and **Baroncini, F.** (2008) Stepwise extinction of larger foraminifers at the Cenomanian-Turonian boundary: a shallow-water perspective on nutrient fluctuations during Oceanic Anoxic Event 2 (Bonarelli Event). *Geology*, **36**, 715–718.

Paytan, A., **Kastner, M.**, **Campbell, D.** and **Thiemens, M.H.** (2004) Seawater sulfur isotope fluctuations in the Cretaceous. *Science*, **304**, 1663–1665.

Pearce, M.A., **Jarvis, I.** and **Tocher, B.A.** (2009) The Cenomanian-Turonian boundary event, OAE2 and palaeoenvironmental change in epicontinental seas: new insights from the dinocyst and geochemical records. *Palaeogeogr. Palaeoclimatol. Palaeoecol.*, **280**, 207–234.

Peucker-Ehrenbrink, B. and **Ravizza, G.** (2000) The marine osmium isotope record. *Terra Nova*, **12**, 205–219.

Pogge von Strandmann, P.A.E., **Jenkyns, H.C.** and **Woodfine, R.G.** (2013) Lithium isotope evidence for enhanced weathering during Oceanic Anoxic Event 2. *Nature Geosci.*, **6**, 668–672.

Pomerol, B. (1983) Geochemistry of the Late Cenomanian-Early Turonian Chalks of the Paris Basin: manganese and carbon isotopes in carbonates as paleooceanographic indicators. *Cretaceous Res.*, **4**, 85–93.

Poulton, S.W., **Henkel, S.**, **März, C.**, **Urquart, H.**, **Flögel, S.**, **Kasten, S.**, **Sinninghe Damsté, J.S.** and **Wagner, T.** (2015) A continental-weathering control on orbitally driven redox-nutrient cycling during Cretaceous Oceanic Anoxic Event 2. *Geology*, **43**, 963–966.

Pratt, L.M., **Force, E.R.** and **Pomerol, B.** (1991) Coupled manganese and carbon-isotope events in marine carbonates at the Cenomanian-Turonian boundary. *J. Sed. Petrol.*, **61**, 370–383.

Prokoph, A., **Babalola, L.O.**, **El Bilali, H.**, **Olagoke, S.** and **Rachold, V.** (2013) Cenomanian-Turonian carbon isotope stratigraphy of the Western Canadian Sedimentary Basin. *Cretaceous Res.*, **44**, 39–53.

Sageman, B.B., **Meyers, S.R.** and **Arthur, M.A.** (2006) Orbital time scale and new C-isotope record for Cenomanian-Turonian boundary stratotype. *Geology*, **34**, 125–128.

Schlanger, S.O. and **Jenkyns, H.C.** (1976) Cretaceous oceanic anoxic events: causes and consequences. *Geol. Mijnbouw*, **55**, 179–194.

Schlanger, S.O., **Arthur, M.A.**, **Jenkyns, H.C.** and **Scholle, P.A**. (1987) The Cenomanian–Turonian Oceanic Anoxic Event, I. Stratigraphy and distribution of organic carbon-rich beds and the marine d13C excursion. In: *Marine Petroleum Source Rocks* (Eds J. Brooks and A.J. Fleet), *Geol. Soc. London Spec. Publ.*, **26**, 371–399.

Scholle, P.A. and **Arthur, M.A.** (1980) Carbon isotope fluctuations in Cretaceous pelagic limestones: potential stratigraphic and petroleum exploration tool. *AAPG Bull.*, **64**, 67–87.

Sinninghe Damsté, J.S., **van Bentum, E.C.**, **Reichart, G.-J.**, **Pross, J.** and **Schouten, S.** (2010) A CO_2 driven cooling and increased latitudinal temperature gradient during the mid-Cretaceous Oceanic Anoxic Event 2. *Earth Planet. Sci. Lett.*, **293**, 97–103.

Sinton, C.W. and **Duncan, R.A.** (1997) Potential links between ocean plateau volcanism and global ocean anoxia at the Cenomanian-Turonian boundary. *Econ. Geol.*, **92**, 836–842.

Snow, L.J., **Duncan, R.A.** and **Bralower, T.J**. (2005) Trace element abundances in the Rock Canyon Anticline, Pueblo, Colorado, marine sedimentary section and their relationship to Caribbean plateau construction and oxygen anoxic event 2. *Paleoceanography*, **20**, PA3005. doi: 10.1029/2004PA001093.

Timofeeff, M.N., **Lowenstein, T.K.**, **da Silva, M.A.** and **Harris, N.B.** (2006) Secular variation in the major-ion chemistry of seawater: evidence from fluid inclusions in Cretaceous halites. *Geochim. Cosmochim. Acta*, **70**, 1977–1994.

Tribovillard, N., **Algeo, T.J.**, **Baudin, F.** and **Riboulleau, A.** (2012) Analysis of marine environmental conditions based on molybdenum-uranium covariation – application to Mesozoic paleoceanography. *Chem. Geol.*, **324–325**, 46–58.

Tsikos, H., **Jenkyns, H.C.**, **Walsworth-Bell, B.**, **Petrizzo, M.R.**, **Forster, A.**, **Kolonic, S.**, **Erba, E.**, **Premoli Silva, I.**, **Baas, M.**, **Wagner, T.** and **Sinninghe Damsté, J.S.** (2004) Carbon-isotope stratigraphy recorded by the Cenomanian-Turonian Oceanic Anoxic Event: correlation and implications based on three key localities. *J. Geol. Soc. London*, **161**, 711–719.

Turgeon, S. and **Brumsack, H.-J.** (2006) Anoxic vs dysoxic events reflected in sediment geochemistry during the Cenomanian-Turonian Boundary Event (Cretaceous) in the Umbria–Marche Basin of central Italy. *Chem. Geol.*, **234**, 321–339.

Turgeon, S. and **Creaser, R.A.** (2008) Cretaceous Oceanic Anoxic Event 2 triggered by a massive magmatic episode. *Nature*, **454**, 323–326.

Voigt, S., **Wilmsen, M.**, **Mortimore, R.N.** and **Voigt, T.** (2003) Cenomanian palaeotemperatures derived from the oxygen isotopic composition of brachiopods and belemnites: evaluation of Cretaceous palaeotemperature proxies. *Int. J. Earth Sci.*, **92**, 285–299.

Voigt, S., **Gale, A.S.** and **Flögel, S**. (2004) Midlatitude shelf seas in the Cenomanian-Turonian greenhouse world: temperature evolution and North Atlantic circulation. *Paleoceanography*, **19**, PA4020. doi: 10.1029/2004PA001015.

Voigt, S., **Erbacher, J.**, **Mutterlose, J.**, **Weiss, W.**, **Westerhold, T.**, **Wiese, F.**, **Wilmsen, M.** and **Wonik, T.** (2008) The Cenomanian – Turonian of the Wunstorf section – (North Germany): global stratigraphic reference section and new orbital time scale for Oceanic Anoxic Event 2. *Newsl. Stratigr.*, **43**, 65–89.

Walker, J.C.G. (1986) Global geochemical cycles of carbon, sulfur and oxygen. *Mar. Geol.*, **70**, 159–174.

West, O.L.O., **Leckie, R.M.** and **Schmidt, M**. (1998) Foraminiferal paleoecology and paleoceanography of the Greenhorn Cycle along the southwestern margin of the Western Interior Sea. In: *Stratigraphy and Palaeoenvironments of the Cretaceous Western Interior Seaway* (Eds W.E. Dean and M.A. Arthur), *SEPM Concepts Sedimentol. Paleontol.*, **6**, 79–99.

Westermann, S., **Vance, D.**, **Cameron, V.**, **Archer, C.** and **Robinson, S.A.** (2014) Heterogeneous oxygenation states in the Atlantic and Tethys Oceans during Oceanic Anoxic Event 2. *Earth Planet. Sci. Lett.*, **404**, 178–189.

Wilmsen, M., **Niebuhr, B.**, **Wood, C.J.** and **Zawische, D.** (2007) Fauna and palaeoecology of the Middle Cenomanian *Praeactinocamax primus* event at the type locality, Wunstorf quarry, northern Germany. *Cretaceous Res.*, **28**, 428–460.

Wright, J., **Seymour, R.S.** and **Shaw, H.F.** (1984) REE and Nd isotopes in conodont apatite: variations with geological age and depositional environment. *GSA Spec. Pap.*, **196**, 325–340.

Zheng, X.-Y., **Jenkyns, H.C.**, **Gale, A.S.**, **Ward, D.J.** and **Henderson, G.M.** (2013) Changing ocean circulation and hydrothermal inputs during Ocean Anoxic Event 2 (Cenomanian–Turonian): evidence from Nd-isotopes in the European shelf sea. *Earth Planet. Sci. Lett.*, **375**, 338–348.

Zheng, X.-Y., **Jenkyns, H.C.**, **Gale, A.S.**, **Ward, D.J.** and **Henderson, G.M.** (2016) A climatic control on reorganization of ocean circulation during the mid-Cenomanian event and Cenomanian-Turonian Oceanic Anoxic Event (OAE 2): Nd isotope evidence. *Geology*, **44**, 151–154.

Zhou, X., **Jenkyns, H.C.**, **Owens, J.D.**, **Junium, C.K.**, **Zheng, X.-Y.**, **Sageman, B.B.**, **Hardisty, D.S.**, **Lyons, T.W.**, **Ridgwell, A.** and **Lu, Z.** (2015) Upper ocean oxygenation dynamics from I/Ca ratios during the Cenomanian-Turonian OAE 2. *Paleoceanography*, **30**, 510–526.

Manuscript received 17 January 2016; revision accepted 29 June 2016